Cerebral Cortex February 2010;20:365-382
doi:10.1093/cercor/bhp107
Advance Access publication July 13, 2009

Duration of Coherence Intervals in Electrical Brain Activity in Perceptual Organization

Andrey R. Nikolaev[1,2], Sergei Gepshtein[1,3], Pulin Gong[1,4] and Cees van Leeuwen[1]

[1]Laboratory for Perceptual Dynamics, RIKEN Brain Science Institute, Wako-shi 351-0198, Japan, [2]Laboratory for Human Higher Nervous Activity, Institute of Higher Nervous Activity, Moscow 117485, Russia, [3]Vision Center Laboratory, Salk Institute for Biological Studies, La Jolla, CA 92037, USA and [4]School of Physics and Faculty of Medicine, University of Sydney, Sydney, NSW 2006, Australia

We investigated the relationship between visual experience and temporal intervals of synchronized brain activity. Using high-density scalp electroencephalography, we examined how synchronized activity depends on visual stimulus information and on individual observer sensitivity. In a perceptual grouping task, we varied the ambiguity of visual stimuli and estimated observer sensitivity to this variation. We found that durations of synchronized activity in the beta frequency band were associated with both stimulus ambiguity and sensitivity: the lower the stimulus ambiguity and the higher individual observer sensitivity the longer were the episodes of synchronized activity. Durations of synchronized activity intervals followed an extreme value distribution, indicating that they were limited by the slowest mechanism among the multiple neural mechanisms engaged in the perceptual task. Because the degree of stimulus ambiguity is (inversely) related to the amount of stimulus information, the durations of synchronous episodes reflect the amount of stimulus information processed in the task. We therefore interpreted our results as evidence that the alternating episodes of desynchronized and synchronized electrical brain activity reflect, respectively, the processing of information within local regions and the transfer of information across regions.

Keywords: EEG, extreme value distribution, perceptual ambiguity, perceptual grouping, quasi-stable synchrony pattern

Introduction

Gustav Theodor Fechner coined the term "inner psychophysics" referring to the scientific pursuit of a lawful relation between neural processes and sensation. This relationship has remained elusive in the following over 150 years. Some progress has been made in animal studies, relating sensory stimulation to spiking activity of cortical neurons. For example, studies of the visual system in behaving animals showed that elementary sensory decisions at the threshold of visibility could be reduced to activity of populations of sensory neurons on the scale from single cells to hundreds of cells (e.g., Parker and Newsome 1998). But even slightly more complex sensory tasks engage very large populations of cortical neurons. Our aim is to bring the elusive goal of inner psychophysics for large neuronal populations one step closer, by introducing and testing a general assumption about how these populations process information.

Large-scale brain activity has been studied using such methods as magneto- or electroencephalography (EEG) and functional tomography. High temporal resolution methods have been particularly illuminating. They showed how different sensory and perceptual processes are associated with "oscillatory" activity in large populations of neurons, for example, with amplitude of oscillations in different frequency bands of electrical brain activity; for alpha band: (Klimesch, Sauseng, and Hanslmayr 2007; Palva S and Palva JM 2007); beta and gamma bands: (Tallon-Baudry and Bertrand 1999; Sannita 2000); or with synchrony of oscillatory activity within and between brain structures (Singer 1999; Varela et al. 2001). But no consensus has been reached on what aspects of the oscillatory activity are relevant for sensation and perception.

Most observations have been interpreted using information-processing approaches that view neural mechanisms as input–output systems. In studies of perception, for example, event-related desynchronization in EEG signals is often taken as a sign that stimulation has engaged a neural mechanism, so subsequent resynchronization is taken to express the disengagement (Pfurtscheller and Aranibar 1977; Pfurtscheller et al. 1994). This view is incomplete because it disregards the dynamics of ongoing (spontaneous) neural activity.

Parameters of ongoing activity vary across time, representing the variability of neural activity and, consequently, the fluctuations of alertness or arousal. Growing evidence shows that ongoing activity significantly affects how animals (Arieli et al. 1996) and humans (Romei et al. 2007) respond to sensory stimulation. Ongoing activity may carry information which the animal (or human) has already learned about the stimulation (Kravitz and Peoples 2008) and therefore may reflect active (although not necessarily specific) anticipation of stimuli. However, in psychophysical experiments, anticipation is typically minimized such that ongoing activity could be treated as mere variability.

Variability in ongoing activity is not random but has a characteristic dynamical structure, expressed by alternation of irregular and regular episodes. These episodes emerge, hold, and dissipate on different temporal scales and in different brain structures (Friston 2000; Freeman et al. 2003; Gong et al. 2003; Stam et al. 2003; Ito et al. 2005). The regular episodes take the form of patterns of phase synchrony, which on the largest spatial scale appear as standing or traveling waves (Ito et al. 2005, 2007). The underlying dynamics can be characterized by collective phase synchronization of neural assemblies near the critical transition to mutual entrainment (Gong et al. 2007). This type of dynamics exhibits remarkable flexibility such that external stimulation can trigger a transfer of neural activity into different phase synchrony patterns with minimal expenditure of energy (cf., Freeman 2007).

van Leeuwen (2007) proposed that neural systems maintain their flexible dynamics across transitions from ongoing to evoked activity. (Note that we use a term "evoked" in a general sense, referring to any type of stimulus-related activity which is superimposed on ongoing activity. In this sense, our use of this term is different from that by Galambos [1992] and

Tallon-Baudry and Bertrand [1999] who attributed evoked only to activity phase locked to the stimulus, as opposed to "induced"—nonphase-locked activity.) If that is the case, then characteristic alternations of the episodes of irregular, desynchronized activity and episodes of synchronized activity are expected in both ongoing and evoked activity. Thus, the theory relating perception to brain activity should be grafted on the properties of ongoing brain activity. On this view, evoked processes constitute a reorganization of phase (phase resetting) in the ongoing activity. Indeed, phase resetting is often thought of as a mechanism generating event-related potentials (ERP) (Brandt et al. 1991; Basar 1999; Barry et al. 2000; Makeig et al. 2002; Hanslmayr et al. 2007).

Let us consider how stimulus presentation affects brain dynamics. When a complex system such as the brain dwells near a critical transition, a $1/f$ signature (or scale-freeness) emerges in brain activity. This signature has been observed in amplitude fluctuations of 10- and 20-Hz oscillation (Linkenkaer-Hansen et al. 2001), as well as in "durations" of synchronized activity (Gong et al. 2003). When a system is perturbed, however, its scale-freeness may be suppressed. For example, during somatosensory stimulation, the power law exponents for the oscillations of 10- and 20-Hz decrease in comparison to the oscillations of ongoing activity (Linkenkaer-Hansen et al. 2004). We therefore expect that, in contrast to spontaneous activity, the episodes of synchronized activity will have characteristic durations in the evoked response paradigm.

The durations of episodes of synchronous activity, rather than other parameters of synchronous activity, should reflect information-processing demands of the task at hand (van Leeuwen et al. 1997). Tyukin et al. (2008) showed that episodes of quasi-stable synchronized activity can represent the outcomes of information processes in a recurrent neural architecture. These episodes have been denoted "coherence intervals" (van Leeuwen and Bakker 1995; van Leeuwen 2007). During these intervals, a mental representation maintains its integrity and its content remains unchanged. This means that no information processing takes place during the interval, whereas the previously processed information is propagated to other brain areas. Such quasi-stable properties are needed to facilitate efficient transfer of information: the oscillations within a coherence interval have to be temporally stable and synchronous because synchrony facilitates communication between neural assemblies (Livanov 1977; von der Malsburg 1985); it helps to keep the temporal "windows of communication" concurrently open for input and output (Fries 2005).

In complex tasks, information is communicated across more areas than in simpler tasks. Multiple information transfers are completed simultaneously within a coherence interval; the time required for completion depends on such factors as cable length, signal transmission capacity, and signal transfer reliability. Yet, the length of a coherence interval is determined by the process that takes longest to complete. For this reason, the more the information transfers must be completed within an interval the longer its expected duration. In addition, because the slowest interval is an extreme value in a random sample, coherence intervals are expected to have an extreme value distribution (Coles and Tawn 1991; Kotz and Nadarajah 2000).

Nikolaev et al. (2005) studied human EEG activity over small regions on the human scalp with an electrode spacing of 2 cm. The authors measured durations of intervals of quasi-stable phase synchrony and found that in the beta frequency range, the intervals were longer when observers were engaged in a perceptual task than when they performed no task. This result was interpreted as evidence that more information was transferred across brain areas in "task" than "no-task" conditions. But the effect of task could be as well driven by such factors as arousal, concentration, and effort. In the present study, we use a more subtle stimulus manipulation to investigate how synchronized brain activity relates to perception.

The closest counterpart to the notion of coherence interval appears in the work of Walter Freeman and colleagues (for a review, e.g., see Freeman 2007). Freeman advanced the hypothesis that intervals of synchronized neural activity emerge as part of a macroscopic action–perception loop, in which early stages of action initiate a corollary discharge to sensory areas of the brain. The corollary discharge prepares sensory areas for settling into a characteristic pattern of synchronized activity (attractor), which then governs the quasi-stable spatiotemporal patterns of brain activity. Such patterns are observed following stimulus presentation; they constitute sequences of events characterized by amplitude modulation of the carrier wave in the gamma or beta frequency range. These patterns have variable durations, followed by sudden phase shifts.

Freeman and colleagues observed that patterns of synchronized activity are specific (but not invariant) to the context of stimulation. Such patterns were observed in animal studies, in olfactory, visual, auditory, and somatosensory cortices (Freeman and Baird 1987; Barrie et al. 1996; Freeman and Barrie 2000; Freeman 2005). In humans, evidence of such patterns has been indirect because neural activity has been recorded using scalp EEG. For example, Freeman et al. (2003) observed quasi-stable synchrony patterns in the beta and gamma frequency range, which were demarcated by abrupt phase changes lasting for about 5 ms. These phase changes occurred with a frequency in the theta or alpha frequency range. The correlation distance of such patterns on the human scalp extended to the entire length of the chains of electrodes (up to 19 cm). The difference in the spatial scale of these synchrony patterns in humans and animals suggests that the sources of these events differ across species (although they may have a common functional significance still, as argued by Freeman 2007).

Freeman and colleagues have not considered the possibility that quasi-stable periods of synchronized activity reflect the amount of transferred information. In contrast, the theory of coherence intervals predicts that durations of these intervals should be directly related to the amount of transferred information. In psychophysical task conditions where stimulus information is systematically varied, we should observe effects of stimulus information on the length of the coherence interval. We presently test this prediction by studying temporal properties of electrical cortical activity in a visual grouping task: we ask whether the amount of "stimulus information" is associated with durations of coherence intervals.

Several studies have explored the relationship between the amount of information contained in visual stimuli and observer performance in perceptual grouping tasks. In particular, van Leeuwen and van den Hof (1991) and Kubovy and Wagemans (1995) measured information content of visual stimulus using Shannon's measure of information. They showed that in ambiguous stimuli, the amount of Shannon's information covaries with stimulus ambiguity. (The entropy of stimulus X, which can be perceived n ways and whose percepts $x_1, \ldots, x_n$

have probabilities $P(x_1), \ldots, P(x_n)$, is $H=\sum_{i=1}^{n} P(x_i)\log[1/P(x_i)]$. Stimuli with the highest entropy convey the least information and vice versa. Thus, the more ambiguous a stimulus [i.e., the more its multiple percepts approach equiprobability, $P(x_i) = 1/n$] the less information it conveys.) For example, Kubovy and Wagemans (1995) investigated perceptual grouping by proximity (Wertheimer 1912; Kubovy et al. 1998) using "multistable dot lattices" (Fig. 1). The amount of stimulus information in dot lattices depends on their "aspect ratio" (AR): the ratio of 2 shortest interdot distances. When the AR of a lattice is at its lowest (which is 1.0), the competing perceptual groupings are equally likely, and Shannon's information content of the lattice is low. In contrast, when the AR is high (larger than 1.0), one of the groupings is more likely to be perceived than the other groupings, and lattice information content is high.

In the present study, we used ambiguous dot lattices in a perceptual grouping task. We evaluated observer performance using a phenomenal report paradigm (Kubovy et al. 1998). We controlled the ambiguity (and thus the information content) of dot lattices by varying their ARs. Because ambiguous lattices contain less stimulus information than the unambiguous lattices, we expected to find an association between lattice ARs and durations of coherence intervals: shorter durations in perception of ambiguous than unambiguous stimuli. In agreement with this expectation, we found that durations of synchronized activity were linearly related to AR (a stimulus property) and that the durations depended on "observers' sensitivity to proximity" (a property of observer). Both factors relate coherence intervals directly to the amount of stimulus information. We also found that the onsets and offsets of coherence intervals were associated with the time course of stimulus presentation. The best-fitting theoretical distributions of the durations were extreme value distributions, in agreement with the theory of coherence intervals. We reproduced these results in 2 experiments in different groups of observers. (The ERP results from these studies were reported elsewhere: for Experiment 1, Nikolaev et al. [2007]; for Experiment 2, Nikolaev et al. [2008].)

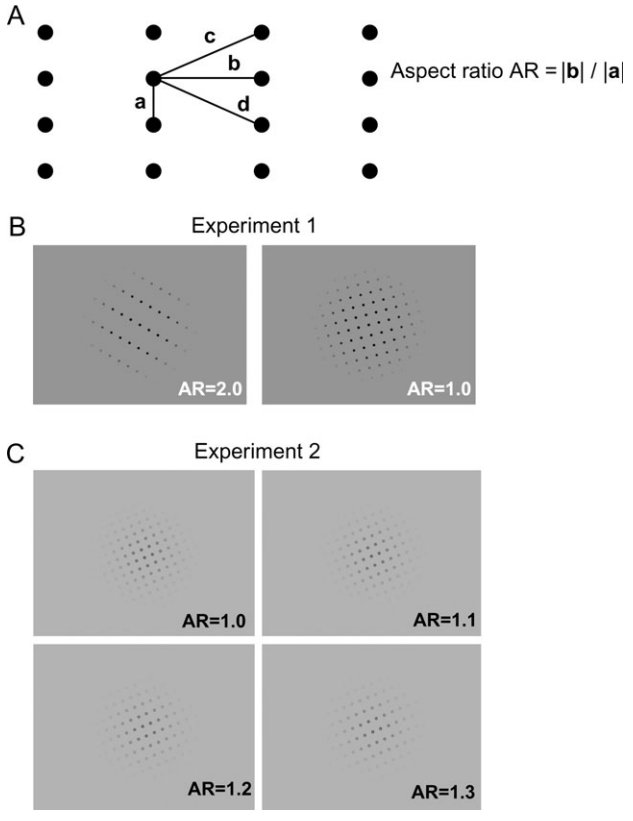

Figure 1. Stimuli used in Experiments 1 and 2. (*A*) Grouping of dots in a lattice depends on its "ARs": the ratio of the shortest and longest distances between the dots. (*B*) Dot lattices of ARs 1.0 and 2.0 used in Experiment 1. (*C*) Dot lattices of ARs 1.0, 1.1, 1.2, 1.3 used in Experiment 2.

Materials and Methods

Experiment 1

Participants

Nine healthy participants (aged 19–33 years, median age 22, 6 women) took part in the experiment. They were all right handed, had normal or corrected-to-normal vision, and were not informed about the purpose of the experiment. Prior to the experiment, all had given their informed consent. RIKEN BSI Institutional Review Board No. 2 (Research Ethics Committee) had approved this study.

Stimuli

We used displays containing dot lattices (Kubovy 1994). The diameter of the dots was 0.15° of visual angle. The shortest interdot distance was 0.8° of visual angle. Dot luminance was modulated in each lattice by a bivariate isotropic Gaussian distribution, such that the dots were visible across a circular area of approximately 7.7° of visual angle in diameter. The background luminance was 51 cd/m^2. The largest Weber contrast of dots was 30% in the lattice center.

The dots on these lattices are spontaneously perceived as grouped into strips. The shorter the distance between the dots in a certain direction the more likely these dots group along that direction. For example, in Figure 1*A*, the 4 most likely perceptual groupings are labeled **a**, **b**, **c**, and **d** according to their proximity: the interdot distances increase from **a** to **d**. We will refer to the corresponding percepts (reports of seeing the groupings) as *a*, *b*, *c*, and *d*. According to the pure distance law (Kubovy et al. 1998), the perceptual grouping of a dot lattice depends on its AR, which is the ratio of the 2 shortest interdot distances, along **a** and **b**.

We used rectangular dot lattices with 2 magnitudes of AR: 1.0 and 2.0 (Fig. 1*B*). At AR = 1.0, the 2 shortest distances were equal to one another; at AR = 2.0, the interdot distance along 1 orientation was twice longer than in the other. We refer to the 2 lattices as AR = 1.0 and AR = 2.0.

Lattices were presented at orientations selected randomly from the following set: 15°, 30°, 60°, 75°, 105°, 120°, 150°, and 165° counterclockwise from the horizontal. For AR = 2.0, this resulted in 8 stimuli, whereas for AR = 1.0, in only 4 stimuli because the following rotations of an AR = 1.0 lattice leave orientation unchanged: 15° and 105°, 30° and 120°, 60° and 150°, and 75° and 165°.

Procedure

Participants were seated at a distance of 1.3 m from the screen in a dimly lit room. Stimuli were presented on an 18-inch TFT Dell monitor using E-Prime software (Psychological Software Tools, Pittsburgh, PA).

Each trial consisted of 4 intervals: fixation, stimulus, blank screen, and response screen. During the fixation, participants were instructed to look at a small circle (0.2° in diameter) presented at the center of an otherwise empty screen for a duration that varied randomly according to a uniform distribution on the interval of 200–600 ms. The durations of the stimulus interval and the blank-screen interval were both fixed at 300 ms. A response screen was presented ad lib, until a response was received. The intertrial interval varied randomly from 1000 to 2000 ms according to a uniform distribution.

Participants reported the orientations of the perceived groupings by choosing 1 of 4 alternatives on the response screen. This screen consisted of 4 circles (response icons), each containing a line tracing a diameter parallel to 1 of the 4 likely grouping directions (**a**, **b**, **c**, or **d**)

of the just-presented lattice. The response alternatives were located in the 4 quadrants of the response screen; their locations were assigned randomly for each trial. Participants responded by pressing 1 of 4 buttons of a response box using their middle and index fingers of both hands. Each button corresponded to 1 of the 4 quadrants of the screen. Because sometimes the perceived grouping switched while the stimulus was on, we asked participants to report the first orientation they perceived after stimulus onset. We advised participants that there was no correct or incorrect answer. The participants learned the procedure in a practice session of 40 trials that preceded the experiment. Each of the 8 AR = 2.0 lattices was presented 12 times, and each of the 4 AR = 1.0 lattices was presented 24 times. The stimuli were presented in random order in blocks of 192 trials. The experiment lasted about 20 min in total.

Experiment 2

Participants

Seventeen healthy participants (aged 19–36 years, median age 22, 9 women) took part in the experiment. All the participants were right handed and had normal or corrected-to-normal vision. All but one of the participants (one of the authors) were unaware of the purpose and design of the experiment. None of the participants but one (MC, not an author) took part in Experiment 1. All participants gave informed consent. RIKEN BSI Institutional Review Board No. 2 (Research Ethics Committee) had approved this study. Four participants were excluded from the analysis: 2 due to EEG artifacts and 2 due to inability to perform the task (see below).

Stimuli

We used dot lattices with 4 values of AR: 1.0, 1.1, 1.2, and 1.3 (Fig. 1*C*). The lattices were presented at 4 orientations, in which the orientation of the shortest distance **a** was rotated counterclockwise from the horizontal for 22.5°, 67.5°, 112.5°, or 157.5°. The 4 ARs and the 4 orientations yielded 16 stimuli. Dot diameter was 0.2° of visual angle. Their luminance was modulated by a bivariate isotropic Gaussian distribution whose maximum was at the center of the lattice (as illustrated in Fig. 1), such that the dots were visible across a circular area with an approximate diameter of 6.9° of visual angle. The distances between dot centers at AR = 1.0° were 0.6° of visual angle. The background luminance was 108 cd/m^2. The largest Weber contrast of dots was 40% in the lattice center.

Procedure

Participants were sitting 1.15 m from the screen in a dimly lit room. The stimuli were presented on a 17-inch CRT display (Eizo FlexScan T566) with an 85-Hz (noninterlaced) refresh rate using E-Prime software.

The task and trial time course were as in Experiment 1, except that the duration of the fixation interval in Experiment 2 was longer (it was randomized between 1200 and 1500 ms) than in Experiment 1, and a different response method was used. In Experiment 2, the participants responded, using a rolling ball device, by clicking on 1 of the 4 "response icons." The cursor was visible only during the response interval.

Each participant practiced the task in a block of 20 trials before the experiment started. Within each experimental block of trials, each of the 16 conditions was presented 10 times in a random order. Four such blocks were presented during an experiment (640 trials in total), which on average took about 1 h, including 3 short breaks (2–5 min long) between the blocks.

Electrophysiological Recording

In both experiments, EEG was recorded using a 256-channel Geodesic Sensor Net (Electrical Geodesics Inc., Eugene, OR). The electrode montage included sensors for recording vertical and horizontal electrooculograms. Data were digitized at 250 Hz. All channels were referenced to the vertex electrode (Cz). Impedance was kept below 50 kOhm. All channels were preprocessed online using 0.1-Hz high-pass and 100-Hz low-pass filtering.

EEG Analysis

The analysis proceeded through 2 main stages: EEG preprocessing and analysis of the duration of synchronized intervals. Our methods in both stages were mostly identical for the 2 experiments, except for some differences as we explain below resulting from differences in difficulty of the grouping task. A detailed presentation of the method and its justification are available elsewhere (Nikolaev et al. 2005). Here we outline its main steps.

Preprocessing was done as follows: we set the epoch of interest for the detection of the synchronized intervals from −100 to +400 ms relative to stimulus onset and considered only the intervals that were fully contained within the epoch. Using a semiautomatic artifact rejection procedure, we excluded the "bad" epochs in which the absolute voltage difference exceeded 50 μV between 2 neighboring sampling points or the amplitude was outside +100 or −100 μV. Two participants of Experiment 2 were excluded because of such bad recordings. We pooled conditions across the orientations because this dimension was irrelevant to the aim of present analysis. As a result, there were about 80–90 "good" epochs per AR condition per participant in Experiment 1 and about 130–150 such epochs in Experiment 2. The data were converted to average reference.

The analysis of synchronized intervals was performed based on single-trial data for each participant, separately for 9 EEG spectral frequencies (see below).

Selection of Areas of Interest

Our choice of areas of interest was motivated by 2 hypotheses 1) that AR affected the strength of perceptual grouping and that the activity of primary visual cortex reflected grouping strength and 2) that the voltage distribution of early ERP components indicated the location of this activity. Because we were using a visual task, we chose our areas of interest and the control areas based on the distribution of voltage maxima of early ERP components in the occipital areas. In a previous ERP analysis, we found that cortical activity in these areas was associated with stimulus AR (Nikolaev et al. 2007, 2008). We searched individual topographical maps for such regions at the latency of ERP components P1 (about 100 ms after stimulus) or N1 (about 200 ms). The area with the largest voltage at either of the 2 latencies was designated as the "peak" area (see inset in Fig. 2). That is, each individual had his or her unique peak area. Within each peak area, we selected a chain of 5 adjacent electrodes, such that the largest ERP amplitude was located under either the second or the third electrode of the chain. We also selected chains of 5 adjacent electrodes in the other hemisphere, in areas symmetric to the peak areas relative to the sagittal plane (to be called "opposite" areas), for permutation statistics in Experiment 1, and in order to control for volume conduction (see below).

In addition to the areas of interest selected in both experiments, in Experiment 1, we also applied our analysis to the left and right temporoparietal areas, the same areas for all the participants. We did so to determine to what extent muscle artifacts contaminated EEG data: electromyogram (EMG) is most prominent in the recordings from the temporal areas. Muscle activity could be correlated with effort, and this could cause differences in synchrony in the high-frequency EEG bands. In particular, in Experiment 1, where the difference between AR conditions was large (AR = 1.0 and 2.0), we expected larger effects than in Experiment 2 (where the differences between AR were small and gradual, ranging from 1.0 to 1.3). It was, therefore, considered sufficient to control for EMG activity only in Experiment 1. Besides serving as a control of muscle artifacts, the comparison of activity in the temporoparietal areas with the activity in our areas of interest (expected to be located in the occipital regions, i.e., over the visual cortex) can provide additional indications of whether our findings reflect effects of visual stimulation.

The scheme map of 256 electrodes in Figure 2 shows the areas of interest defined for individual participants and marks locations of the chains of electrodes selected for analysis.

Detection of Intervals of Quasi-Stable Phase Synchrony

We studied brain connectivity by measuring phase synchronization of cortical activity. Comparative studies of various synchronization measures have shown that the sensitivity of phase synchronization to

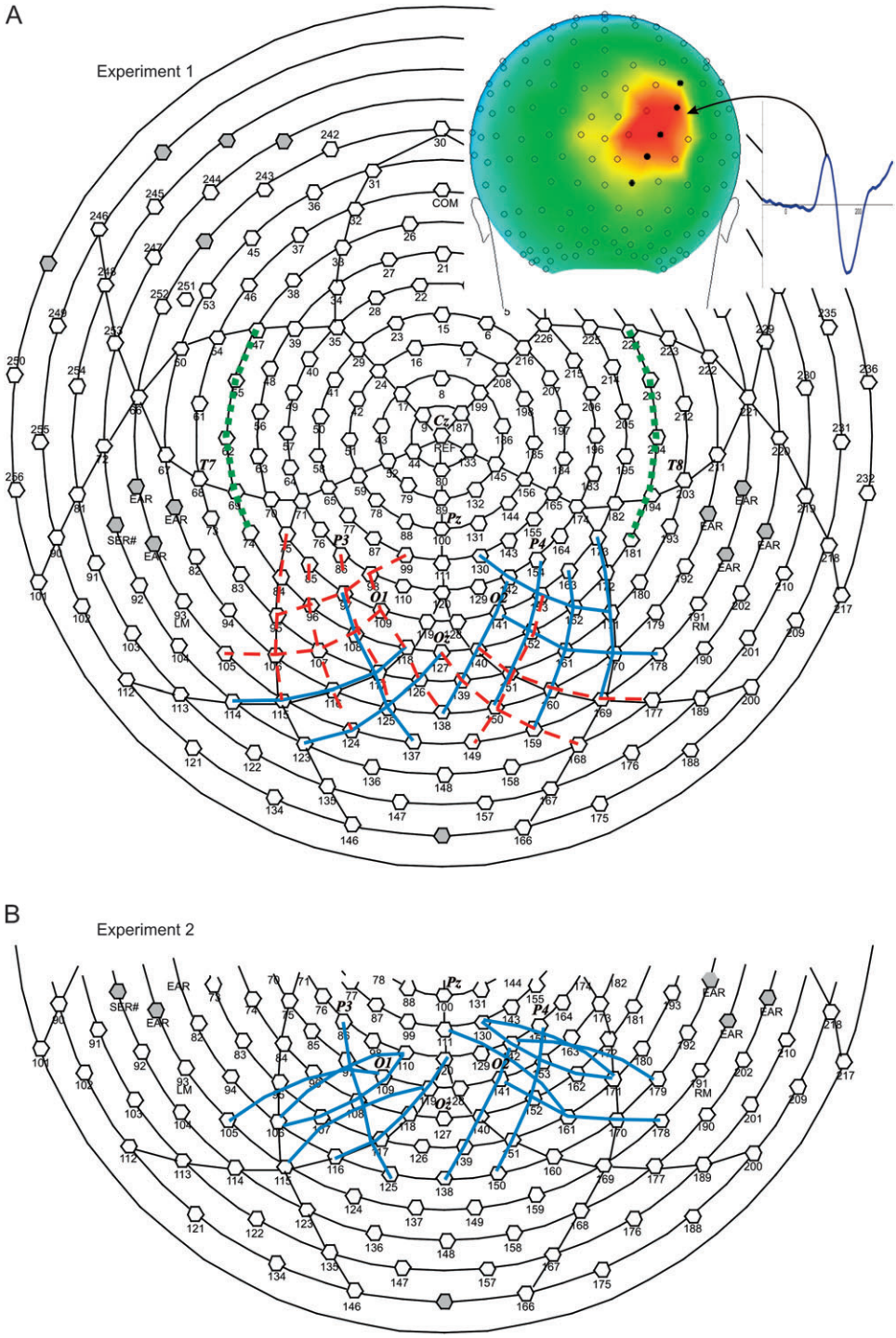

Figure 2. A 256-channel electrical Geodesic Sensor Net with individually selected chains of adjacent electrodes for synchronization analysis. (*A*) Electrode chains for 9 participants in Experiment 1. The chains in the peak areas are marked by blue (solid) lines, and those in the "opposite" areas are marked by red (dashed) lines. The green (dotted) lines designate chains in the right and left temporoparietal (control) areas. (*B*) The chains in the peak areas for 13 participants in Experiment 2. Spacing between electrodes is uniform, which is distorted in the figure because of the polar projection. The labels of landmark electrodes are according to the International 10-20 system of electrode placement. The inset in the right upper corner illustrates how an electrode chain was selected in the peak area on the voltage map at the peak latency of the P1 component.

linear and nonlinear properties of EEG signals is similar to other measures of functional connectivity, such as generalized synchronization, mutual information, and cross-correlation (Quian Quiroga et al. 2002; David et al. 2004). We computed phase synchronization as follows. We obtained the instant phase of EEG signal using a Morlet wavelet transform for 9 central frequencies: 10, 13, 15, 18, 21, 25, 30, 36, and 43 Hz. We used a logarithmic frequency step size because of the scaling property of the wavelet transform. For the frequency of 10 Hz, wavelet duration was 267 ms and spectral width was 2.4 Hz; for the frequency of 43 Hz, wavelet duration was 62 ms and spectral width was 10.3 Hz. We then computed a relative phase difference in pairs of channels. We approached synchronization from a statistical point of view, looking for peaks in distributions of relative phase differences (Tass et al. 1998). We computed a phase synchronization index by

using the first Fourier mode of each such distribution (Rosenblum et al. 2001) (for details, see Nikolaev et al. 2005).

Of the 2 end electrodes in every chain, we chose the one that was closer to the vertex and designated it as the reference for calculating the phase synchronization. For each of the 4 remaining electrodes in the chain, we calculated an index of phase synchronization versus the reference (Fig. 3*A*). We used the standard deviation (SD) calculated across the 4 indices as our main measure. This measure reflects the uniformity of synchronization along chains of electrodes. As a function of time, SD reflects the dynamics of synchronized activity within a region of interest. To compare this dynamics across trials, conditions, and participants, we standardized SD such that the mean of SD distribution is 0 and the SD is 1. In order to identify intervals with uniformly high synchrony in every (local) area, we introduced an SD threshold. A time interval was considered synchronized for a duration in which SD values remained below the threshold. Another threshold was needed, as only intervals longer than some minimal length can be meaningfully related to behavior (Freeman and Barrie 2000; Freeman 2005). We previously found that in human EEG effects of task are observed only when the length exceeded 80 ms (Nikolaev et al. 2005). Thus, we introduced a minimal duration (MD) threshold, in addition to the SD threshold.

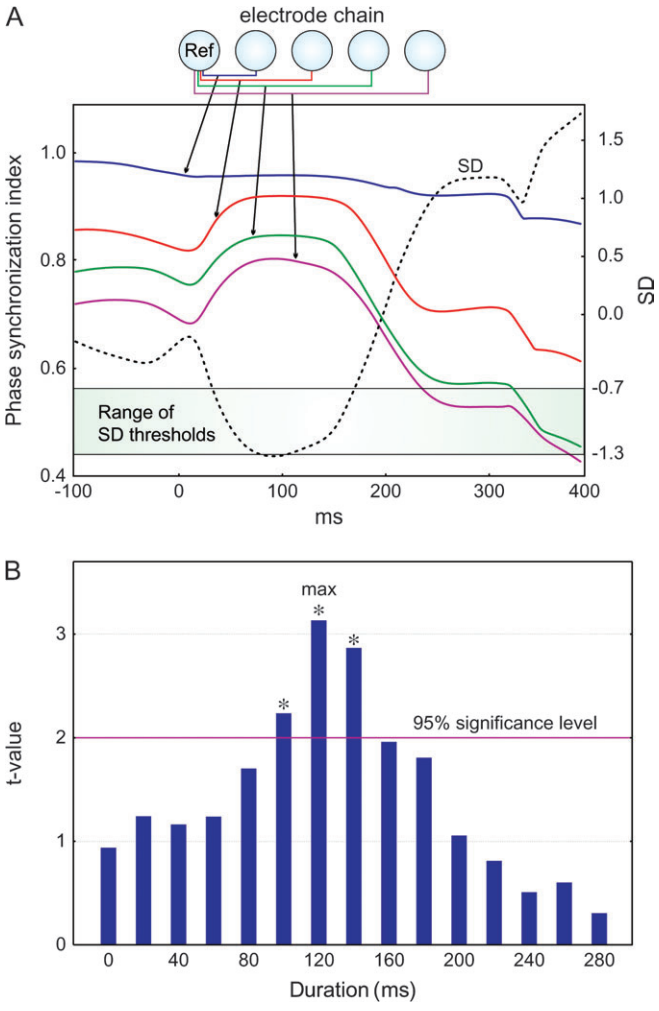

Figure 3. (*A*) Definition and duration estimation of a synchronized interval. On a single trial, 4 pairwise synchronization indices are measured as a function of time in a chain of 5 electrodes (shown schematically on the top). SD across the synchronization indices are computed as a function of time. The synchronized interval is a period during which SD falls below a threshold in the range of thresholds shaded in the figure. (*B*) Example of 1 run of search for differences between conditions at a given SD threshold: the results of 15 sequential *t*-tests with sequential removing of intervals shorter than the values of durations on the abscissa. Significant *t* values summed to obtain a *t*-sum statistic are marked with asterisks. The duration with a maximal behavioral difference is marked "max."

Comparison of Intervals of Quasi-Stable Phase Synchrony between Experimental Conditions

To avoid arbitrariness in choice of threshold values, we evaluated durations of synchronized intervals in a sweep through all possible combinations of SD and MD thresholds, as we describe below. SD and MD thresholds were varied in small steps, and each time, the differences in the durations between conditions were evaluated using a *t*-test. For SD thresholds, the step size was 0.01 and the range was from −0.7 to −1.3 of normalized units; for MD thresholds, the step size was 20 ms and the range was from 0 to 300 ms. The maximally possible synchronized interval duration was 496 ms: the window size (500 ms, from −100 to +400 ms) minus 2 data points.

For each SD threshold value, we calculated a *t*-sum statistic, based on a sweep through all the MD threshold values. The *t*-sum statistics for a given SD threshold was a sum of all the significant *t* values ($P < 0.05$) across all MD thresholds. As we show in Figure 3*B*, we performed 15 such *t*-tests, each test corresponding to a different MD threshold value, to obtain 1 *t*-sum statistic. Only the *t* values marked with an asterisk ($P < 0.05$) were taken into account. The significance of *t*-sum values themselves was evaluated using a permutation procedure described in the next section.

In Experiment 1, we calculated *t*-sum statistics for each SD threshold for duration differences of synchronized intervals in AR = 1.0 and 2.0 conditions, for each area of interest in individual participants. In Experiment 2, we used the AR = 1.0 condition for comparison to each of the other AR conditions (1.1, 1.2, and 1.3).

Testing for Significance

We used a permutation procedure to obtain a distribution of surrogate *t*-sum statistics. This procedure involves randomly exchanging individual pairwise synchronization indices across chains of electrodes between areas (Experiment 1) or conditions (Experiment 2). Surrogate data must contain all EEG features of the original data, except for the feature in question. The large difference between AR conditions in Experiment 1 may produce a large but irrelevant difference in the EEG, which might contaminate the surrogate series. Within conditions, however, these features have to be similar in the opposite areas, that is, areas symmetrically opposite to the peak areas across the sagittal plane. Surrogate data for Experiment 1 were therefore created by randomly exchanging indices between electrode chains in peak and opposite areas for the same trials.

We randomly exchanged entire single-trial time series of synchronization indices recorded between electrodes and the reference in the peak area with ones in the opposite area, separated by an equal distance from the reference (Nikolaev et al. 2005). For instance, the time series from a pair of electrodes separated by 2 cm in the peak area was exchanged with the time series from a corresponding electrode pair in the opposite area also separated by 2 cm. As a result, the permuted set of indices always contained indices for pairwise distances 2, 4, 6, and 8 cm. The numbers of permuted epochs (surrogate trials) matched those in the original data for each participant.

For Experiment 2, the same permutation procedure was used, except that here the differences between AR conditions were considered sufficiently small to use them as the source of surrogate distributions. We therefore permuted synchronization indices, instead of between peak and opposite areas, between the peak areas of AR = 1.0 trials and the peak areas of trials belonging to each of the other AR conditions (1.1, 1.2, and 1.3), respectively, resulting in 3 separate sets of surrogate data for pairwise comparisons between these conditions and the AR = 1.0 condition. Because the surrogates for Experiment 2 were assembled from synchronization indices taken from different trials, this procedure preserved all pairwise phase relations between channels, ongoing as well as evoked, while eliminating any systematic phase relations among pairs of channels (except for the relations which were constant across trials and which were separately evaluated using intertrial coherence, see below). In particular, what is eliminated in these series is any systematicity in SD of the pairwise synchronization indices, on which our measure of synchronized durations is based. In using time series

from different trials, our permutation procedure is similar to the trial-shuffling procedure proposed by Lachaux et al. (1999). But Lachaux et al. continued their analysis by evaluating averages from shuffled trials where we continued our analysis with single trials.

After permutation, we computed for both experiments the SDs across the surrogate synchronization indices, as we did in the main analysis. The permuted data were compared in the same manner as the original data, and *t*-sum statistics were calculated. This procedure was repeated 1000 times for each SD threshold to yield a distribution of permuted *t*-sums. An original *t*-sum was labeled as significant if it exceeded the 95th percentile of the distribution of permuted *t*-sums for a given SD threshold. This analysis was done separately within every frequency and every participant.

Data Reduction and Significance Testing across Participants

We analyzed how durations of synchronized intervals depended on AR across EEG frequencies and areas of interest. These analyses were performed separately for every participant (9 and 13 participants in Experiments 1 and 2, respectively). For each individual and each area of interest, we measured the differences between AR conditions (between AR = 1.0 and AR = 2.0 in Experiment 1 and between AR = 1.0 and, respectively, 1.1, 1.2, and 1.3 in Experiment 2). We tabulated these differences in terms of their *t*-sums at each of 61 SD threshold values for each of 9 frequencies, yielding a 61 × 9 table in Experiment 1 and 3 such tables in Experiment 2. The sign of *t*-sum indicated the direction of these differences: negative (for shorter durations in AR = 1.0 than in AR > 1.0), positive, or 0 (when no significant *t*-sum was observed).

Next, we reduced the 61 × 9 tables to 3 × 1 tables of trinary values (+, –, and 0), as we explain below. The purpose of this reduction was to reveal patterns of differences across observers. The first step of reduction was to replace all the nonsignificant *t*-sum values with zeros based on the results of our permutation analysis. The values in the resulting sparse table were called *t* scores.

In Experiment 1, we selected the maximal absolute *t* score across all SD threshold values for a given frequency. We then summed maximal *t* scores across frequencies for 3 bands: alpha (10 + 13 + 15 Hz), beta (18 + 21 + 25 + 30 Hz), and gamma (36 + 43 Hz). We used the signs of resulting *t* scores as entries in the reduced table.

In Experiment 2, we first selected the entries in the sparse tables for which the *t* scores were nonzero for both conditions AR = 1.2 and 1.3 (disregarding condition AR = 1.1, where nonzero *t* scores were rare). Then, we computed the sum of *t* scores in conditions AR = 1.2 and 1.3 and found the SD threshold at which the sum of *t* scores was maximal. (Different t-sum signs between AR = 1.2 and 1.3 occurred very rarely: in peak areas—in 0.17%, in opposite areas—in 0.01% of all cases [9 frequencies 3 61 thresholds 3 13 participants]. We omitted these cases from the analysis.) For every frequency, we took the *t* scores at this SD threshold from the tables for conditions AR = 1.1, 1.2, and 1.3 and summed them to obtain a new *t* score, which may deviate from the previous value of *t* score because some entries in the AR = 1.1 table may have nonzero values. Then, as in the previous experiment, we combined these values for 3 bands: alpha (10 + 13 + 15 Hz), beta (18 + 21 + 25 + 30 Hz), and gamma (36 + 43 Hz) and used the signs of resulting *t* scores as entries in the reduced table.

For each experiment, we calculated the number of participants with positive and negative signs (i.e., the participants whose durations of synchronized intervals were, respectively, longer and shorter in AR = 1.0 than in AR > 1.0). To estimate the statistical significance of these results, we evaluated how many participants are expected to have the same sign of *t* score by chance and we used a permutation procedure, as follows. Let the data be represented by a 1-dimensional array with values "+," "–," or "0" (the sign of effect for each participant). In the significance test, we randomly filled this array with + and – values with equal probability. Then, we randomly replaced some of these values with 0 values. The number of such 0 values was drawn randomly from a Gaussian distribution. The mean and SD of this distribution were the same as the mean and SD of 0-value distribution in original arrays across frequency bands and areas, separately for Experiments 1 and 2. We repeated this procedure 1000 times. From the resulting distribution of arrays, we found the 95th percentile of the number of values (either positive or negative), which was incidentally 7 in both experiments. (The same 95% percentile value for 2 experiments with different number of participants is explained by larger number of zeros [absence of a significant difference] in Experiment 2, probably because of smaller difference between ARs.) Thus, 8 or more participants with the same sign of the *t*-sum value presented a significant result at the $P < 0.05$ level.

Volume Conduction

Because we analyzed synchronization in chains of electrodes spaced about 2 cm apart, it is important to control whether our measure of synchronization depended on volume conduction of currents through head tissues. (For a detailed discussion of the role of volume conduction in our method, see Introduction in Nikolaev et al. 2005.)

Besides its use in statistical tests, our permutation procedure for generating surrogate synchronization data helps to ensure that our measures of synchronization are independent of the effects of volume conduction. If volume conduction had given rise to systematic temporal variations of synchrony across conditions, the variations would be the same in the peak and opposite occipital areas in Experiment 1 because we see no reason to expect different volume conduction anisotropies in symmetrical cortical areas within the same temporal interval. This way we excluded systematic variation in volume conduction as an explanation of the effect of stimulus AR on synchronized intervals.

In addition, our measure of synchronization benefits from the fact that volume conduction inflates synchronization indices toward the maximally possible values. Because of volume conduction, synchronization indices were the highest in pairs of adjacent electrodes (e.g., the blue and red lines in Fig. 3*A*). Because synchronization indices in these pairs approached the "ceiling" of synchronization, variability across all electrode pairs has the same interpretation: less variability means increase of synchronization and more variability means decrease of synchronization. This way, volume conduction helps to interpret the fluctuations of synchronization.

Results

Behavioral results

Experiment 1

In the biased lattices (AR = 2.0), participants predominantly saw dots grouped along the shortest distance, in organization *a* (96.6 ± 2.2% of responses). The other organizations were perceived at an average response rate of 2.3 ± 1.7% across participants, excluding 1 participant for whom these responses reached 40%. In the unbiased lattices (AR = 1.0), the 2 most likely responses (*a* and *b*) were observed with equal frequency (43.2 ± 5.7% and 44.3 ± 6.1%), whereas the 2 others responses were observed in 12.5 ± 9.3% of trials. The response times (RTs) were as follows: 1562 ms (standard error [SE] = 121 ms) for AR = 1.0 and 1401 ms (SE = 102 ms) for AR = 2.0.

Experiment 2

We excluded 2 participants from the analysis because they were unable to perform the task adequately (as indicated by near-zero grouping sensitivity, see below). In this experiment, the changes of lattice ambiguity across AR conditions were smaller than in Experiment 1. We estimated the effect of AR manipulation by measuring response log-odds:

$$L = \log\{[N(\neg a) + 1/6]/[N(a) + 1/6]\},$$

where $N(a)$ is the number of reports of grouping along **a** and $N(\neg a)$ is the number of other reports (i.e., grouping along **b**, **c**, and **d**) (Kubovy et al. 1998). In Figure 4, we plot *L* versus lattice ARs. The thick lines represent linear fits to the data. Its slope (indicated in the top right corner of each panel) is called

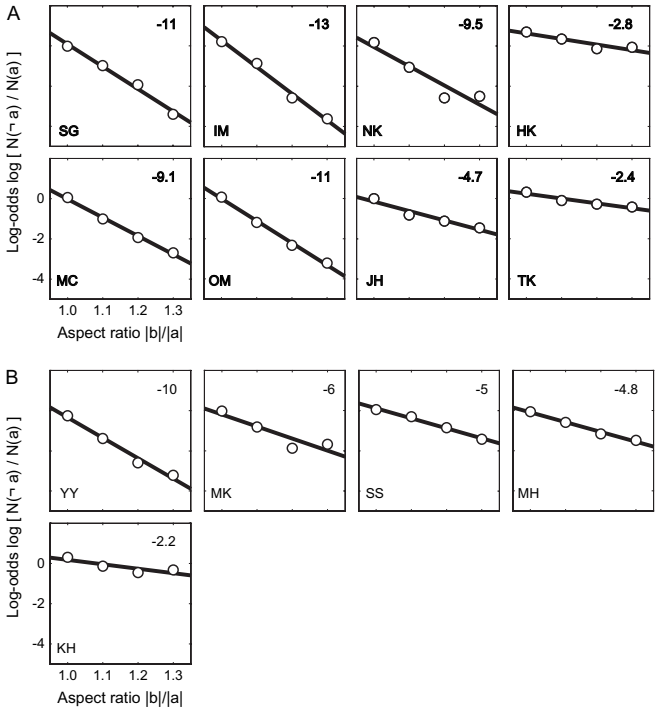

Figure 4. Grouping sensitivity in Experiment 2. In every panel, we plot the log-odds of responses as a function of lattice ARs. The thick lines represent linear fits to the data. The slopes of fits (attraction coefficients indicated in the top right corner of each panel) represent grouping sensitivity. In (*A*), we plot results for participants whose synchronized intervals were systematically related to AR, and in (*B*), we plot results for participants who showed no such relation.

"attraction coefficient." We used absolute values of attraction coefficients to measure "grouping sensitivity," that is, the degree to which responses of individual observers depended on the AR of dot lattices. Large values of this coefficient represent high sensitivity and small values represent low sensitivity. The RTs for AR = 1.0, 1.1, 1.2, and 1.3 were, respectively, 1777, 1773, 1734, and 1754 ms (SE = 68, 57, 61, and 59 ms).

EEG Results

AR Effects on Duration of Synchronized Intervals: Overall Results

Percentages of the participants whose durations of synchronized intervals were, respectively, longer or shorter in AR = 1.0 than in AR > 1.0 are presented in Figure 5. In both experiments, 8 participants had negative scores in the peak areas in the beta band, which exceeds in each experiment the number 7 required for significance (Fig. 5*B*). The negative score indicates shorter durations in AR = 1.0 than in AR > 1.0. In Experiment 1, the remaining participant (1 of 9) had a positive score; in Experiment 2, the remaining 5 of 13 participants had 0 scores. We found no significant effects in cortical areas or frequency bands other than the peak areas in the beta band, although we found 2 tendencies in the opposite areas (Fig. 5*A*,*C*). Figure 5*B* shows that the proportion of participants with shorter durations in AR = 1.0 than AR > 1.0 was about 30% larger in Experiment 1 than in Experiment 2. This is likely an effect of the larger dissimilarity between AR conditions in Experiment 1 than in Experiment 2.

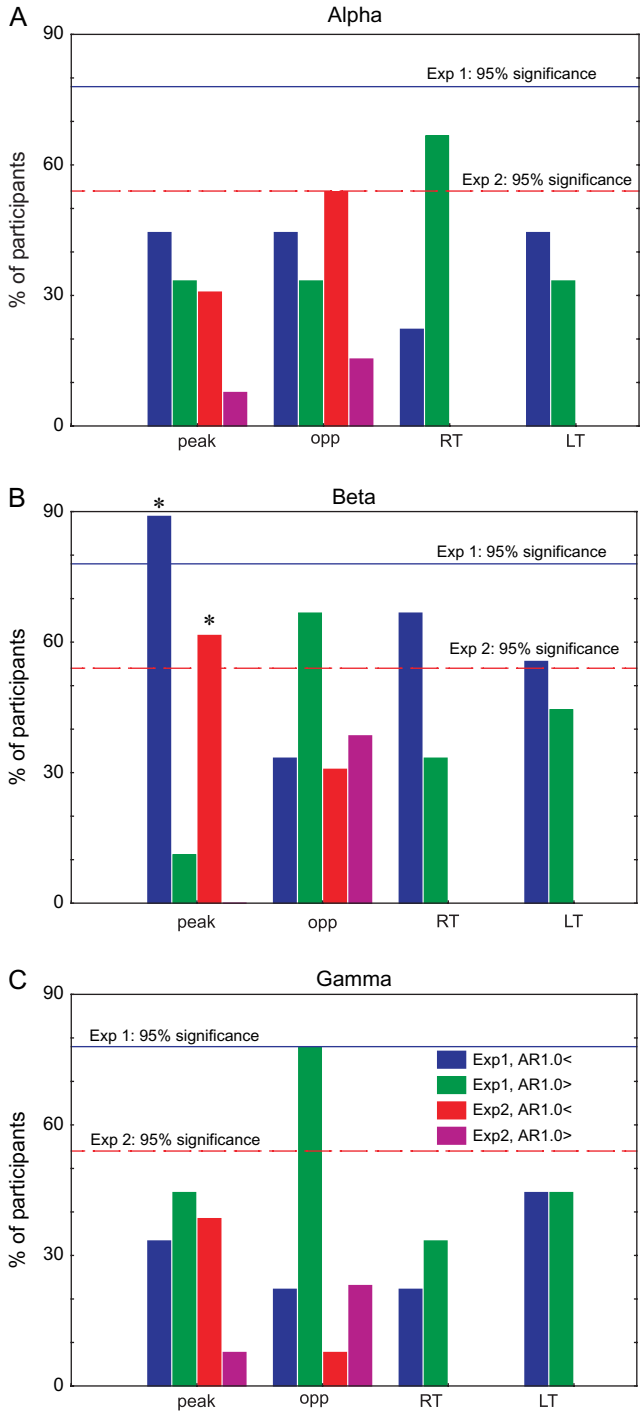

Figure 5. Percentage of participants with longer (AR1.0>) and shorter (AR1.0<) durations in condition AR = 1.0 than in AR > 1.0, for 4 areas in Experiment 1 and for 2 areas in Experiment 2. Data for different frequency bands appear in separate panels: alpha in (*A*), beta in (*B*), and gamma in (*C*). The blue (solid) and red (dashed) horizontal lines represent 95% significance levels computed in the permutation procedures, respectively, in Experiments 1 and 2. The absolute number of participants corresponding to the significance levels in both experiments is 7. The asterisks mark the conditions that exceeded the significance level.

AR Effects on Duration of Synchronized Intervals: Individual Results

Having demonstrated that durations in condition AR = 1.0 are consistently shorter than in condition AR > 1.0 within the beta

band across participants, we next estimated SD thresholds and frequencies responsible for this effect within participants. For those participants who showed an effect of AR in their peak areas, we determined the frequency within the beta band (18, 21, 25, and 30 Hz) and the SD thresholds for maximal *t* scores in Experiment 1. In Experiment 2, we additionally summed *t* scores in conditions AR = 1.2 and AR = 1.3 and selected the maximal values of the results. In Figure 6*A*, we plot the distribution of frequencies within the beta band and in Figure 6*B* the distribution of SD thresholds. Remarkably, the 21-Hz frequency dominated among beta frequencies in both experiments.

For each participant, we estimated the durations of synchronized intervals in which differences between conditions were maximal. In Experiment 1, we found a duration for which the difference between conditions AR = 1.0 and AR = 2.0 was most prominent. At the frequencies and SD thresholds selected as we described above (Fig. 6*A,B*), we consecutively removed the shorter intervals in 20-ms steps, starting from 0 ms, and identified the maximal *t* value among these steps (marked "max" in Fig. 3*B*). The distribution of these "minimum" durations across participants is shown in Figure 6*C*. The mean minimum duration was 75 ms (standard error of the mean [SEM] = 16.4 ms). For the synchronized intervals of which the durations exceeded this value, we computed the mean duration for each participant, which are shown in Figure 7.

Similarly, in Experiment 2, we consecutively removed the shorter intervals with 20-ms step at the frequencies and SD thresholds selected as we described above (Fig. 6*A,B*). Because there were several AR levels in Experiment 2, we had to use a criterion different from the one used in Experiment 1. Now the criterion was the maximal regression coefficient in a linear regression of the durations on the 4 AR conditions. In all but one (S.G.) participants whose difference between conditions AR = 1.0 than in AR > 1.0 was significant, the regression coefficients were positive and significant (for S.G. $P = 0.056$) (Fig. 8*B,C*). These fits indicate a consistent increase of durations of synchronous intervals as a function of AR (Fig. 8*A*). For control purposes, we used the same procedure in the opposite areas. Here, the regression coefficient was significant in 2 participants only (IM and MC; Fig. 8*B,C*). In the peak areas, the overall mean of the minimum durations was 80 ms (SEM = 22.0 ms). The durations of intervals whose durations exceeded minimum value are on the right of Figure 8, averaged across participants.

The durations averaged across participants are shown for each AR for Experiments 1 and 2 in Figure 9. One AR condition (AR = 1.0) was common for both experiments. We asked whether the durations for this AR were comparable in the different groups of participants. The *t*-test revealed that the mean durations in AR = 1.0 did not differ ($t_7 = 0.42$) between Experiments 1 and 2. The difference between the mean durations in AR = 2.0 of Experiment 1 and in AR = 1.3 of Experiment 2 was also insignificant ($t_7 = 0.98$) (Fig. 9), although the durations in AR = 2.0 were on average about 24 ms longer than in AR = 1.3.

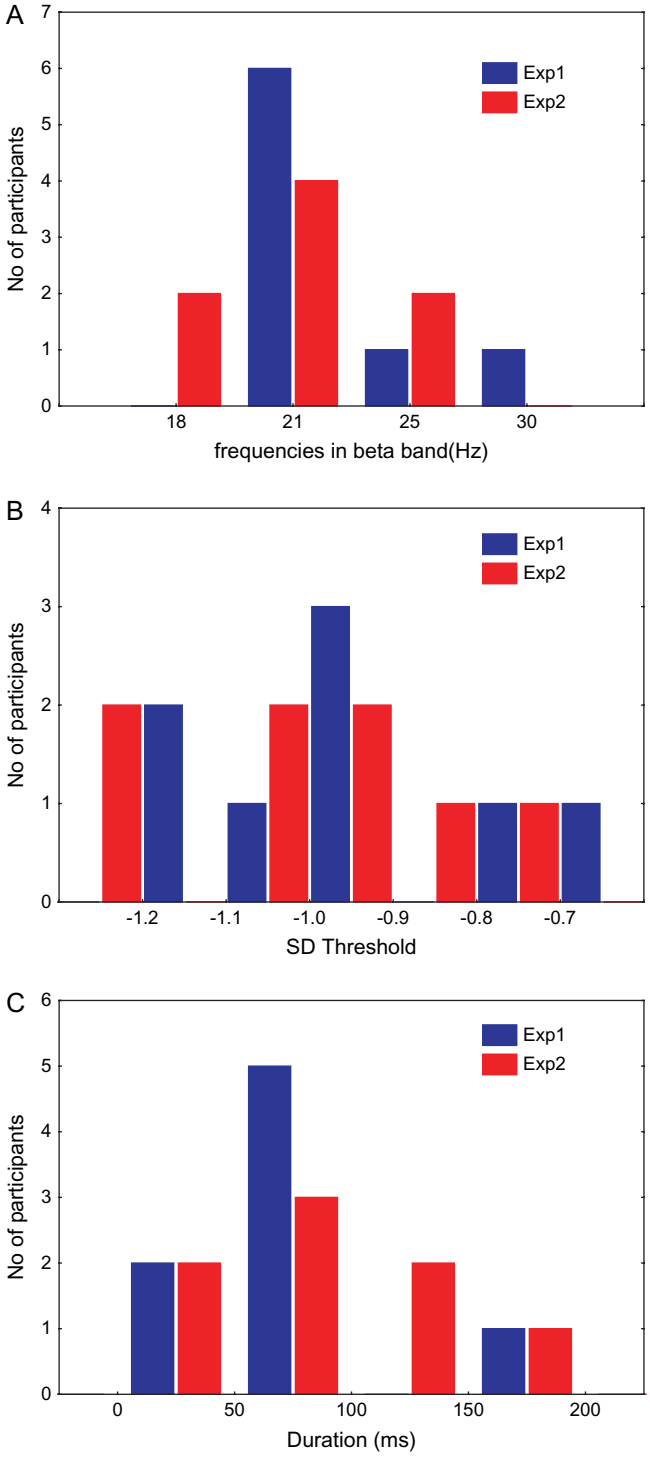

Figure 6. Distributions of frequencies (*A*), SD thresholds (*B*), and minimum durations (*C*) of synchronized intervals corresponding to maximal difference between conditions AR = 1.0 and AR > 1.0 in the 2 experiments.

Contribution of Phase-Locked and Nonphase-Locked Activities to Duration of the Synchronized Intervals

Detection of phase synchronization is sensitive to fluctuations in signal amplitude. We investigated whether evoked signal amplitude could explain the systematic relationship between AR and the duration of synchronized intervals. For the 8 participants in Experiment 2 who showed this relationship, we averaged EEG from the electrode chains selected individually for every participant, as described above (*Selection of areas of interest* and Fig. 2), and obtained their beta frequency amplitudes (Fig. 6*A*) using a complex Morlet wavelet. We extracted activity both phase locked or nonphase locked to the stimulus (Galambos 1992; Tallon-Baudry and Bertrand 1999). To determine the phase-locked activity, we first averaged raw EEG data and then extracted the amplitudes. In order to

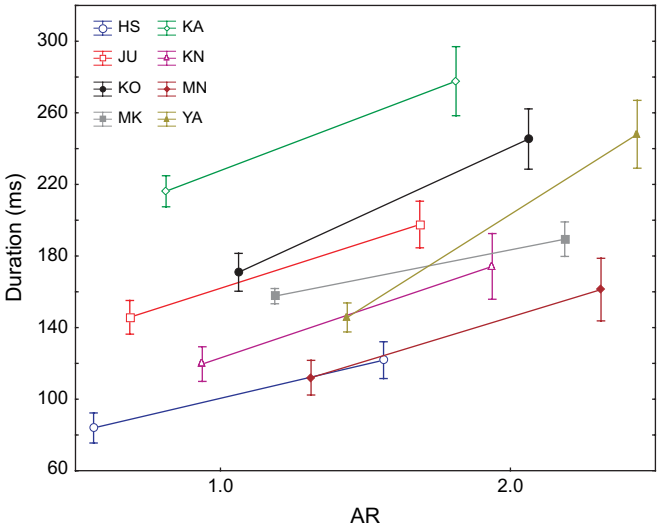

Figure 7. Mean and SEM for durations of synchronized intervals for each participant in the peak areas in Experiment 1.

determine how consistent EEG phase was across trials, we computed the phase-locking factor (Tallon-Baudry et al. 1996) called "intertrial coherence" in the EEGLAB software we used (Delorme and Makeig 2004). Intertrial coherence is an additional control of our permutation procedure: it is a measure of phase-locked activity, which was constant across trials and to which our permutation procedure was not sensitive. To study nonphase-locked activity, we first computed the wavelet amplitudes of beta activity in single trials and then averaged the results across trials. We evaluated the amplitude and intertrial coherence as a function of AR (4 levels) by repeated-measures analysis of variance (ANOVAs) for each time point of the epoch in the interval of −100 to +400 ms using the Huynh–Feldt correction to compensate for violation of sphericity. In addition, we tested the possible linear dependency of amplitude or intertrial coherence on AR, similar to that of synchronized interval durations. We used as a post hoc test a pointwise linear regression of amplitude and intertrial coherence on AR (1.0, 1.1, 1.2, and 1.3). We considered only those time points where the *P* levels in both ANOVA and regression were below 0.05. To take into account the effect of multiple comparisons, we considered only cases where the significance level of $P < 0.05$ was reached in both ANOVA and regression for at least 11 consecutive samples.

For "phase-locked" activity, amplitude reflected AR in the interval of 230–254 ms after stimulus presentation (Fig. 10*A,D*), but the regression did not reveal a linear relationship with AR. The intertrial coherence had a prominent peak at about 100 ms (Fig. 10*B,E*) but was not related to AR here, nor elsewhere in the epoch.

For "nonphase-locked" activity, amplitude reflected AR in intervals before and immediately after stimulus presentation (Fig. 10*C*). In the first interval, from −70 to −18 ms (demarcated by vertical lines in Fig. 10*C*), regression showed a linear relationship with AR, with larger amplitude for AR = 1.0 and smallest for AR = 1.3 (Fig. 10*F*), opposite to what would have been expected if AR led to an increase of the nonphase-locked response. The duration of this interval (52 ms) was shorter than the minimal threshold for synchronized interval (80 ms). This

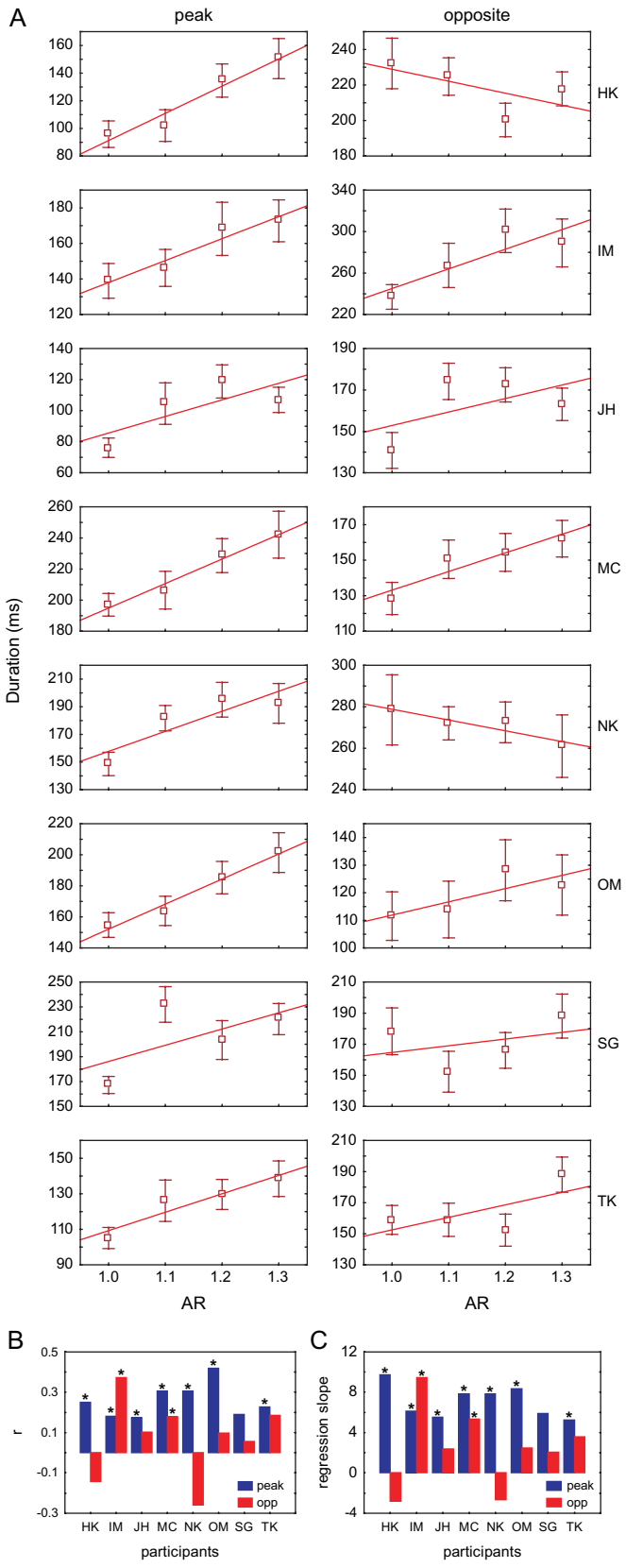

Figure 8. (*A*) Mean and SEM for durations of synchronized intervals in the peak and opposite areas in Experiment 2 for the participants in whom we found shorter durations in AR = 1.0 than in AR > 1.0. The line in every panel represents a linear regression fit to the data. The regression coefficients of the slopes are plotted, respectively, in (*B*) and (*C*).

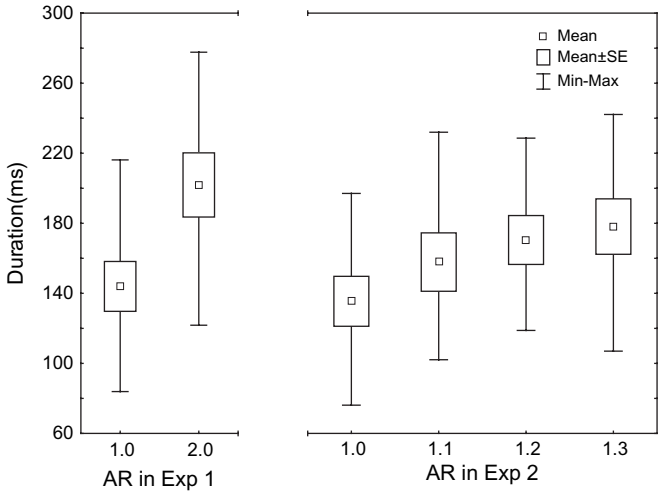

Figure 9. Mean, SEM, and the range of durations of synchronized intervals averaged across 8 participants in whom we found shorter durations in AR = 1.0 than in AR > 1.0 in the 2 experiments.

interval happened prior to stimulus presentation, and participants could not possibly have predicted the AR of the stimuli. Thus, the linear relationship in this first interval must have occurred by chance. Consistent with this conclusion, data from individual participants did not show linear trends, in contrast with the synchronized interval durations, where the trends reached significance in individual participants (Fig. 8). In the second significant ANOVA interval, from 22 to 64 ms after stimulus presentation, the relationship between amplitude and AR was not linear even in the averages (Fig. 10*G*).

To summarize, we found evidence that neither the amplitude of phase-locked, nor nonphase-locked beta activity, nor the intertrial coherence could explain the relationship between AR and synchronized interval durations.

Distribution of Task-Related Synchronized Intervals

According to the theory of coherence intervals, length of the interval is determined by the slowest process in communication between brain areas. It is therefore expected that interval lengths should follow an extreme value distribution. To test this prediction, we analyzed distributions of durations that were longer than the minimum duration (i.e., durations relevant to perception). We compared these distributions with a large set of parametric distributions (using EasyFit software, MathWave Technologies). We excluded from this analysis all the distributions that had more than 3 parameters. We fitted the remaining 38 theoretical distributions 1) to the individual data and 2) to the pool of data collected across all participants within each experiment. We evaluated the goodness of fit using the Kolmogorov–Smirnov test and ranked theoretical distributions according to the results of this test. In the individual fits, we averaged the ranks across participants. In Table 1, we present results for the 3 top-ranked distributions. The generalized Pareto and generalized extreme value distributions competed for the first rank. Kolmogorov–Smirnov statistics of the 3 distributions were highly insignificant (Fig. 11*B*,*D*). This result means that the fits were excellent so that the empirical and theoretical distributions were statistically indistinguishable.

Most of the distributions featured in Table 1 are adequate descriptions of extreme events. Generalized Pareto distribution, which is at the first position in the mean individual ranks, is widely used to model extreme events (Hosking and Wallis 1987; Coles and Tawn 1991). Extreme value distributions comprise Gumbel and Weibull families (as well as Fréchet-type distributions) (Kotz and Nadarajah 2000). The Weibull distribution is a generalization of the Rayleigh distribution (Mudholkar and Srivastava 1993). Therefore, it is likely that the observed distributions of interval durations are extreme value distributions, in agreement with predictions of the theory of coherence intervals (Fig. 11*A*,*C*). (Because truncating the lower part of our empirical distribution could result in a bias for the extreme value distribution, we replicated the analysis with all the intervals, including the shortest ones. The result shows that generalized Pareto distribution in Experiments 1 and 2 was at the first position among 38 ranked distributions for both mean individual ranks and fitting durations pooled over participants.)

Onset and Offset of the Synchronized Intervals

In a previous study (Nikolaev et al. 2005), we had contrasted synchronized intervals that were shorter and longer than the MD and found they differ in their onset and offset latencies. We report about these onset and offset latencies in our present data. We derived the distribution of onset and offset latencies in ten 50-ms bins in the epoch of 500-ms length (–100 to +400 ms). However, for the long intervals, the number of onsets in the "end of an epoch" and the number of offsets in the "beginning of an epoch" had to be small because of a small number of intervals that reached the end of an epoch for onsets or terminated in the beginning of an epoch for offsets. (We considered only the intervals fully contained within –100 to +400 ms of the stimulus onset.) Therefore, the number of onsets in the end (and offsets in the beginning) of an epoch could not be measured reliably. To evaluate the lengths in those parts of an epoch where the onsets or offsets could not be measured, we calculated the 95th percentile of the distribution of long intervals. The 95th percentile was 300 ms in Experiment 1 and 296 ms in Experiment 2. The 300 ms amounted to six 50-ms bins. Accordingly, we did not use the last 6 bins for onsets (and the first 6 bins for offsets) in these measurements. Instead, we evaluated the onsets in 4 bins from –100 to +100 ms, and the offsets in 4 bins from 200 to 400 ms.

Distributions of onsets and offsets averaged across participants are shown in Figure 12. To evaluate the number of onsets and offsets as a function of latency, we performed a repeated-measures ANOVA with factors interval length (short vs. long) and time Bin (4 levels). These were performed separately for onsets and offsets and for each experiment.

In Experiment 1 for onsets, the effect of interval length was significant, $F_{1,7} = 7.3$, $P < 0.05$, and the effect of time bin and the interaction were not significant (Fig. 12*A*). A post hoc least significant difference test showed a smaller number of onsets in the bin 50–100 ms (marked with an asterisk in Fig. 12*A*) than in the preceding bins –100 to 50 ms ($P < 0.05$) and 0–50 ms ($P = 0.05$). For offsets, the effect of interval length approached significance, $F_{1,7} = 5.0$, $P = 0.06$, and the effect of time bin and the interaction were not significant. But the number of offsets for the long intervals gradually increased starting from the bin of 250–300 ms, the difference with which approached significant in

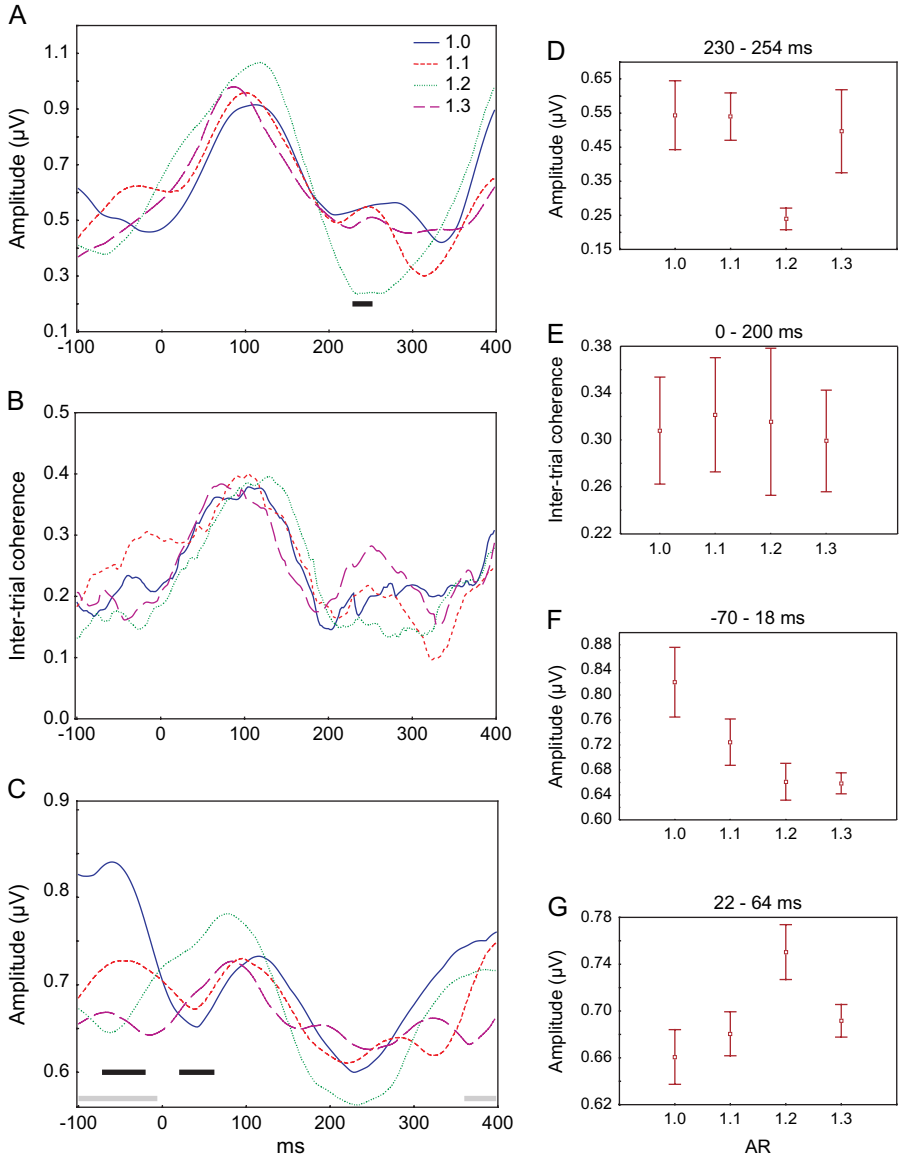

Figure 10. (*A*) Grand-average amplitude of phase-locked beta activity for the 4 ARs. (*B*) Grand-average intertrial coherence for the 4 ARs. (*C*) Grand-average amplitude of nonphase-locked beta activity for the 4 ARs. The horizontal bars indicate intervals of significant AR effects: according to pointwise ANOVAs (black) and according to pointwise regressions (gray). (*D*) Mean and SEM of the phase-locked amplitude in the interval of 230–254 ms after stimulus, shown in (*A*). (*E*) Mean and SEM of the intertrial coherence in the interval of 0–200 ms after stimulus. (*F*, *G*) Mean and SEM of the nonphase-locked amplitude in the intervals from 70 to 18 ms before stimulus onset and 22–64 ms after stimulus onset, shown in (*C*).

Table 1
Ranked estimates of goodness of fit of theoretical distributions to observed distributions of synchronized interval durations

Mean rank			Pooled		
	Rank	Statistics		Rank	Statistics
Experiment 1					
Generalized Pareto	4.5	0.100	Generalized extreme value	1	0.029
Generalized extreme value	6.9	0.111	Rayleigh (2P)	2	0.030
Gumbel max	9.6	0.118	Fatigue life (3P)	3	0.031
Experiment 2					
Generalized Pareto	1.6	0.048	Generalized extreme value	1	0.022
Weibull (3P)	5.1	0.061	Rayleigh (2P)	2	0.025
Generalized extreme value	6.1	0.065	Weibull (3P)	3	0.026

Note: The first 3 ranks among the 38 tested distributions are shown, for the ranks averaged across individual fits (mean rank) and pooled across all the participants within an experiment (pooled).

the bins of 300–350 ($P = 0.08$) and 350–400 ms ($P < 0.05$) (Fig. 12*A*).

In Experiment 2 for onsets, we found a significant effect of interval length, $F_{1,7} = 42.1$, $P < 0.001$, and a tendency for the effect of time bin, $F_{3,21} = 2.5$, $P = 0.09$, Huynh–Feldt $\varepsilon = 1$ (Fig. 12*B*). The interaction was not significant. A post hoc test showed a smaller number of onsets in the bin 0–50 ms (marked with an asterisk in Fig. 12*B*) than in the preceding bin –50 to 0 ms ($P < 0.05$). For offsets, the effect of interval length was significant, $F_{1,7} = 20.8$, $P < 0.01$, the effect of time bin approached significance, $F_{3,21} = 2.7$, $P = 0.07$, Huynh–Feldt $\varepsilon = 1$, and the interaction was not significant. A post hoc test showed that relative to the bin 200–250 ms (marked with an asterisk in Fig. 12*B*), the number of offsets increased in the following bins 250–300 ($P = 0.05$) and 350–400 ms ($P = 0.07$).

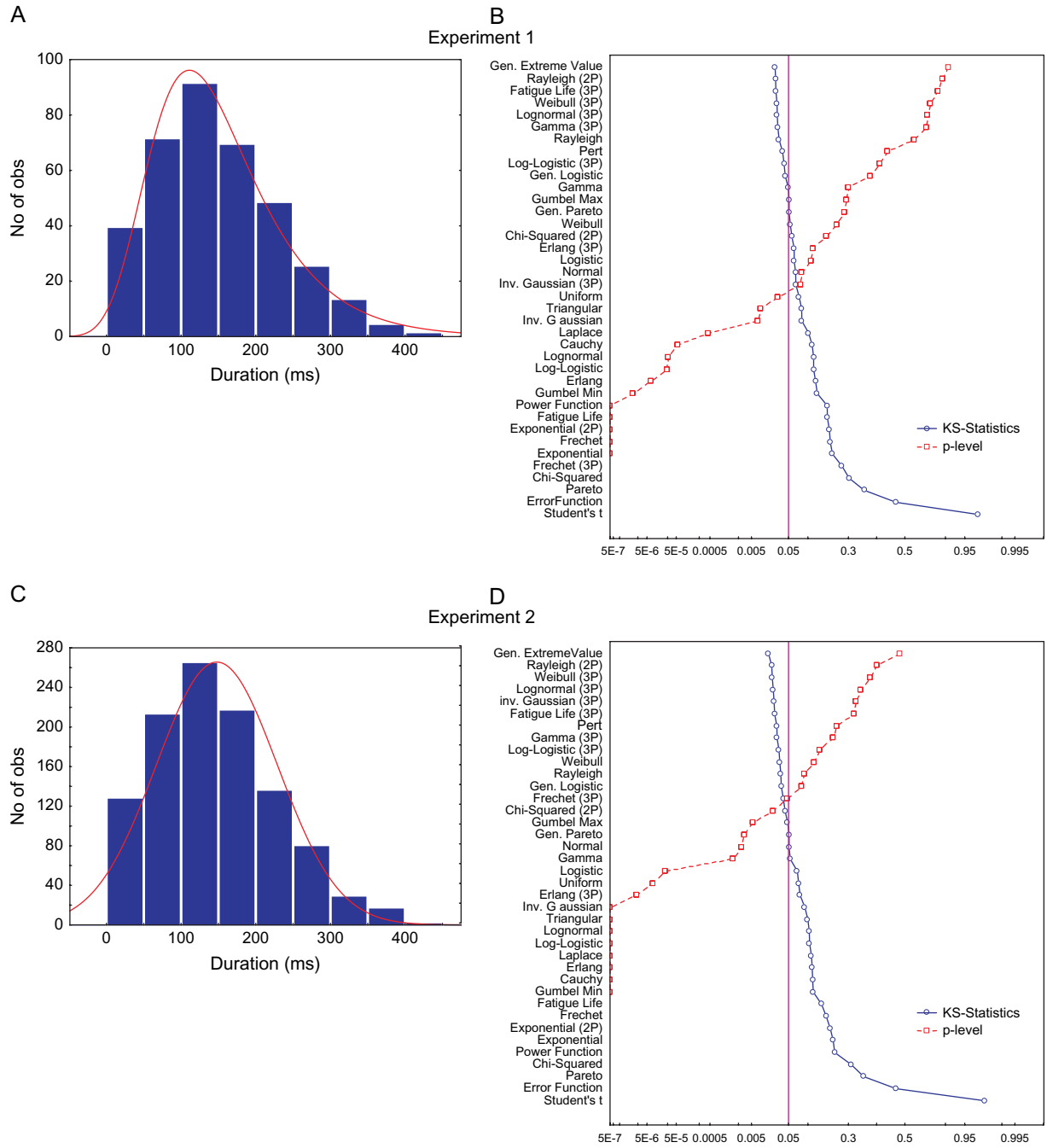

Figure 11. (*A*, *C*) Duration distributions of the synchronized intervals (pooled over participants) that were longer than the MD in Experiment 1 (*A*) and Experiment 2 (*B*). The red curve is the fit of the generalized extreme value distribution. (*B*, *D*) The Kolmogorov–Smirnov (KS) statistic and the corresponding *P* levels for 38 distributions in Experiment 1 (*C*) and Experiment 2 (*D*). The vertical line designates 0.05 significant *P* level.

The results are consistent across the 2 experiments for the long intervals. Their frequency of onsets decreased immediately after stimulus presentation. Onsets reached a minimum 1 bin later in Experiment 1 than in Experiment 2. The frequency of offsets increased after the bin of 250–300 ms, which corresponded to the moment of stimulus removal.

Synchronized Interval Durations and Individual Grouping Sensitivities

To understand why high ARs corresponded to longer durations of synchronized intervals, in Experiment 2, we examined how these durations related to individual grouping sensitivities reflected in attraction coefficients (Fig. 4). We performed a multiple regression analysis of single-trial durations with 2 predictors: attraction coefficient and AR (multiple regression, $R^2 = 0.16$; overall goodness of fit, $F_{2,1075} = 101.8$, $P < 1 \times 10^{-17}$). Regression coefficients were highly significant for both attraction coefficient (0.36, $t = 12.7$, $P < 1 \times 10^{-17}$) and AR (0.18, $t = 6.5$, $P < 1 \times 10^{-9}$). In Figure 13, we plot individual averaged durations as a function of grouping sensitivity for each AR condition. This plot shows that, just as we found for high AR, long durations are associated with high attraction coefficients.

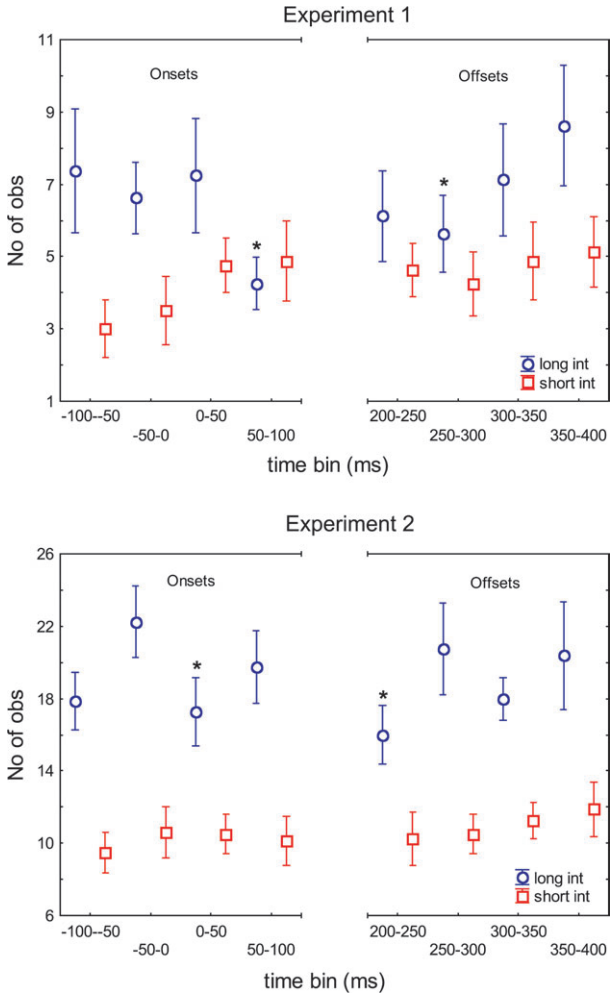

Figure 12. Frequencies of the onsets and offsets (mean ± SEM) of synchronized intervals that were longer or shorter than the minimum duration for Experiment 1 (*A*) and Experiment 2 (*B*). Significant changes of frequency relative to neighboring bins are marked by asterisks.

We also averaged durations of synchronized intervals for each participant across trials and performed a multiple regression analysis of the averaged durations with 2 predictors: attraction coefficient and AR. The multiple regression accounted for about half of the variance ($R^2 = 0.55$, overall goodness of fit, $F_{2,29} = 17.7$, $P < 0.00001$). Regression coefficients were significant for both attraction coefficient: 0.65 ($t = 5.2$, $P < 0.0001$) and AR: 0.36 ($t = 2.9$, $P < 0.01$).

Discussion

We studied synchronized electrical brain activity in local regions of the scalp of human observers engaged in a perceptual grouping task. The task was to report the orientation of the perceived groupings in dot lattices. We found that the "duration" of synchronized activity in the beta frequency band depended on the ambiguity of stimulation and on individual grouping sensitivity. These dependencies were observed for synchronized intervals that exceeded a minimal duration (MD) of about 80 ms. This result is consistent with the observation of Freeman and Barrie (2000) that only synchronized intervals longer than some MD were related to behavior.

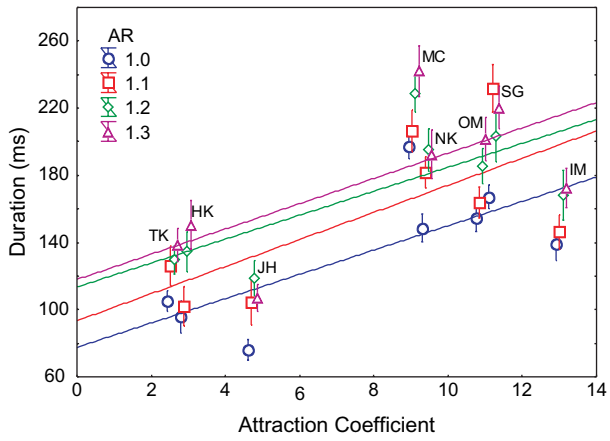

Figure 13. Correlation between attraction coefficients (which measure grouping sensitivity; Fig. 4) and durations of synchronized intervals (mean ± SEM) for each AR condition in the group of 8 participants in Experiment 2.

Effect of Stimulus Ambiguity

Synchronized brain activity depended on the degree to which a stimulus organization dominated perception within a trial. Durations of the intervals of synchronized activity depended on 2 factors, both associated with perceptual ambiguity: one was a property of stimulation (aspect ratio, AR, of dot lattices) and the other was a property of participant (grouping sensitivity):

1. AR of dot lattices controls how strongly the most likely perceptual organization is supported by stimulus geometry (Fig. 1): the higher the AR the more dominant is that interpretation the lower is stimulus ambiguity. In both Experiments 1 and 2, we observed longer durations of synchronized intervals for biased (AR > 1.0) than ambiguous (AR = 1.0) stimuli. Notably, in Experiment 2, the graded increase of AR was associated with a graded prolongation of synchronized intervals (Figs 8 and 9).
2. Grouping sensitivity reflects how much participant's preference of the dominant organization depends on the AR (Fig. 4). Participants with high grouping sensitivity report the dominant organization more often than participants with low grouping sensitivity. We found that high grouping sensitivity was associated with long synchronized intervals (Fig. 13).

AR corresponds to graded perceptual ambiguity, that is, to uncertainty, or lack of information in the perceptual judgment. Dot lattices with high ARs contain more information for the grouping task than lattices with low ARs (Kubovy and Wagemans 1995). Individual sensitivity, or the lack thereof, equally reflects uncertainty with respect to stimulus information. These results, therefore, are consistent with the view that the lengths of coherence intervals reflect the amount of information communicated across different parts of the visual system.

According to the theory of coherence intervals, periods of synchrony are the periods during which communication between brain structures takes place. Because the slowest process determines length of the coherence intervals, the intervals are expected to have an extreme value distribution. In accordance with this prediction, we found that the generalized Pareto and extreme value distributions competed for the best-fitting theoretical distributions of the durations of synchronized intervals (Fig. 11).

Reaction times (RTs) were longer in ambiguous than in nonambiguous stimuli. A likely reason is that in ambiguous stimuli, observers tended to vacillate between response alternatives, consistent with the notion that stimulus uncertainty of ambiguous stimuli was high. Note the opposite trends in the associations of 1) RT and stimulus ambiguity and 2) durations of synchronized intervals and stimulus ambiguity. We therefore conclude that the effect of stimulus ambiguity on RTs is mediated by a mechanism unrelated to the mechanism that controls the durations of synchronized intervals.

Can the results be explained by attractor dynamics, which, according to Freeman and colleagues, governs the evolution of a quasi-stable synchronized neural activity? One could argue, for instance, that perceptual switching between alternative organizations of an ambiguous stimulus is a manifestation of switching between alternative attractor states of neural activity (e.g., Ditzinger and Haken 1990). Then, perhaps, competition between the attractor states would somehow be reflected in the durations of intervals of synchronized activity. But this argument is inconsistent with the well-known properties of attractor dynamics: a system governed by an attractor follows a specific path in the state space toward the attractor and this process is not expected to depend on other possible system states, including attractors, outside of this path (van der Helm 2006).

EEG Frequency Band of Synchronized Intervals

Our findings on synchronized activity in relation stimulus and individual properties were specific to the beta frequency band (18–30 Hz) (Figs 5*B* and 6*A*). This observation is consistent with previous results (Nikolaev et al. 2005) and with numerous reports about the association of cortical activity in the beta band with visual perception. For example, perception of gratings presented in different visual hemifields was accompanied by increase of interhemispheric coherence in the beta band when the gratings were co-oriented rather than orthogonal to one another (Knyazeva et al. 1999, 2006). In binocular rivalry, cortical interactions in the beta band were associated with perception of alternating stimuli (David et al. 2004). Beta-band synchronization was also associated with perception of semantic aspects of visual perception (von Stein et al. 1999), target detection in attentional blink (Gross et al. 2004), object recognition (Supp et al. 2005), and visual short-term memory (Tallon-Baudry et al. 2001).

We found no association between perception and duration of synchronized intervals in other frequency bands, including the gamma band (Fig. 5*C*), where other studies have reported correlation between synchronous activity and feature binding (reviewed in Singer 1999; Tallon-Baudry and Bertrand 1999). This discrepancy may be explained by a systematic relationship between sizes of synchronized networks and the frequency band of their synchronization: the higher the frequency the smaller the size (von Stein and Sarnthein 2000). Gamma-band synchronization is generally responsible for local communication across short cortical distances, whereas beta frequencies can synchronize over longer conduction delays, that is, between more distant brain structures (Kopell et al. 2000). Thus, it is plausible that the significance of beta band in our results is a consequence of the spatial scale of our measurements (about 8 cm).

Freeman (2005) distinguished between 2 types of synchronized patterns related to stimulus presentation. The first pattern has a carrier frequency in the gamma band; it appeared soon after stimulus presentation and persisted for relatively short time. This pattern is modality specific and localized over the primary sensory cortex. The second pattern has a carrier frequency in the beta range; it appeared later (but it might also occur in prestimulus epochs) and lasted longer than the gamma pattern. The beta pattern was synchronized over the primary sensory cortex and subcortical areas. Although these patterns were found in animal studies, that is, at a different spatial scale than here, the properties of the beta pattern make it more likely to be detected in scalp EEG than the gamma pattern. It is therefore the beta pattern that probably corresponds to the pattern of synchronized activity observed presently.

Time Course of Synchronized Activity

Task-relevant synchronized intervals (i.e., intervals > 80 ms) often began prior to stimulus presentation (Fig. 12) (cf., Lachaux et al. 2000; Freeman 2005). This activity may reflect preparatory behavior. Nonspecific preparation may occur under conditions of random variation of stimuli with impoverished semantics typical for psychophysical experiments. Recruitment of ongoing activity helps to meet resource demands during stimulus processing (Nakatani et al. 2005). Synchronized intervals continued in the transition from ongoing to evoked activity. Of the evoked activity, neither phase-locked nor nonphase-locked amplitudes showed a systematic relationship to ARs (Fig. 10*A*,*C*; The linear relationships between the amplitude of the nonphase-locked activity and ARs [Fig. 10*C*] observed before stimulus presentation were not confirmed in the individuals and were shorter the MD of 80 ms above which ARs were associated with the duration of synchronized intervals.). This is evident that the relationship between synchronized interval duration and AR occurred because of changes in phase rather than amplitude.

We distinguished 2 types of activity phase locked to the stimulus. The first type involved stable phase relations between channels that were constant across trials. This type of activity was not eliminated in the surrogates, and therefore, we evaluated it by intertrial coherence (or phase-locking factor; Tallon-Baudry et al. 1996). We found a peak of the intertrial coherence at about 100 ms after stimulus onset (Fig. 10*B*). This result suggests that "phase resetting" of ongoing activity may occur at this instant, in response to stimulus presentation. The timing of phase resetting may be functionally significant (Gruber et al. 2005; Klimesch, Hanslmayr, et al. 2007). Instantaneous phase locking may help to maintain exact timing of information processing in the brain, by establishing temporal windows during which neural systems are prepared for particular information-processing tasks (Tallon-Baudry and Bertrand 1999; Klimesch et al. 2006; Fell 2007).

The abrupt phase change overlaps with ERP components C1 and P1, with latencies 60–110 ms. Other findings in the present data (reported in Nikolaev et al. 2008) showed that components C1 and P1 reflected effects of AR and grouping sensitivity. In general, oscillations of different frequencies that are phase locked to the stimulus can contribute to the generation of ERP components in a manner specific to the behavioral task (Klimesch, Hanslmayr, et al. 2007). For example, in a memory retrieval task, phase alignment of alpha-band activity significantly contributed to generation of the P1 component and phase alignment of (mainly) theta-band activity

contributed to generation of the N1 component (Gruber et al. 2005). ERP components may also be associated with high-frequency activity: phase-locked high-frequency oscillations were shown to be negatively correlated with component N70 (C1) and positively correlated with component P100 (P1) (Sannita et al. 1995).

However, the abrupt phase changes at the 100-ms latency were not associated with AR, in contrast to the amplitude of the low-frequency ERP components. Possible reasons are the following: 1) the phase changes happened in a narrow frequency band around 20 Hz (see the previous section of Discussion) in contrast to the wide band ERP response and 2) effects of AR on C1 and P1 amplitude were too small or too short lived to have a measurable effect on the signal-to-noise ratio and, consequently, on the estimates of phase synchrony.

Besides the fact that this type of phase-locked activity coincided with early ERP components, the phase-locked activity also coincided with an abrupt decline in the onset frequency of task-relevant synchronized intervals (Fig. 12). The phase-locked activity, therefore, appears to interfere with the synchronization. Nikolaev et al. (2005) observed a similar drop in onsets at a later stage, coinciding with ERP component N1 with a 200-ms latency. This component was associated with differences between task and no-task conditions and therefore was understood to reflect the deployment of task-specific attention. In the current experiments at about 100 ms after stimulus, the early ERP components, the peak of intertrial coherence, and the drop in onsets all coincided. This moment may demarcate the beginning of the perceptual grouping process.

The second type of phase-locked activity is characterized by stable phase relations between channels that vary across trials (Lachaux et al. 1999). It is therefore not visible in the intertrial coherence. However, within a trial, the phase relations are stable and persist for some duration. This mechanism is supposed to support the synchronization of activity across brain regions. For example, phase locking within rhinal cortex and hippocampus may trigger rhinal–hippocampal synchronization related to memory formation (Fell et al. 2008). The function of this mechanism is to facilitate communication across regions. This type of phase-locked activity may therefore give rise to systematic effects among pairs of channels that were eliminated in the surrogates of Experiment 2. Against this background, the effect of AR on synchronized interval durations was observed. Therefore, the AR effect to a considerable degree depends on this second type of phase-locked activity.

This type of phase-locked activity might be necessary for the effects of synchronized interval durations, but could it also be sufficient? Phase-locked oscillations are usually short term, widespread over brain areas, and broadband (Yeung et al. 2004). The present effects were not short term: in the intervals shorter than 80 ms, we did not find a systematic effect of their duration on AR. Also, the association of grouping sensitivity and durations of synchronized intervals was observed only in the intervals that were longer than 80 ms. The mean duration of synchronized intervals was 140–180 ms (Figs. 7 and 9), and some of them lasted until stimulus offset (300 ms after stimulus presentation) (Fig. 12). Nor were the effect broadband or widespread: we found them only in a narrow beta band (Fig. 6*A*) and in the peak areas (Fig. 2). We therefore consider the contribution of activity with stable phase relations (between channels) that are nonphase locked to the stimulus. We cannot exclude that this activity forms characteristic patterns among pairs, which we have identified as synchronized intervals. Assuming that phase-locked activity was not sufficiently long lived to sustain these intervals, we set our cards on a synergistic effect of phase-locked and nonphase-locked activities.

Implications for Mechanisms of Cortical Communication

As we mentioned in the Introduction, intervals of synchronized activity (coherence intervals) could manifest information transfer between brain structures (van Leeuwen and Bakker 1995; van Leeuwen 2007): the more information is transferred and the more brain structures get involved the longer the synchronized intervals. This argument led to the predictions we tested in the present work.

The quasi-stable synchrony patterns observed in visual, auditory, and somatic cortices (Barrie et al. 1996; Ohl et al. 2001; Freeman 2005) are sometimes presented as evidence of discrete processing of information in the brain. (Freeman 2007, dubbed these patterns "cinematographic frames.") The notion of discrete processing originated in psychology (Lalanne 1876; von Uexkuell 1928). It enjoyed some popularity in experimental psychology in 1950–70s (Stroud 1955; Lichtenstein 1961; Kristofferson 1967; Geissler 1987), and now it undergoes a revival (reviewed in VanRullen and Koch 2003; Palva S and Palva JM 2007). Although our findings are not inconsistent with the notion of discrete processing, they do not commit us to the view that information processing occurs in discrete stages. Coherence intervals are relatively local events, so many coherence intervals may co-occur at different locations in the brain. These intervals may overlap in time to various degree, yielding a continuous flow of information across the brain. The question of whether cortical processing is discrete or continuous (in the above sense) can be perused in future studies aimed at discovering the temporal organization of multiple coherence intervals.

Notes

We thank Peter Jurica, Tatiana Tyukina, and George Fedorov for technical support and Lars Strother for generating the stimuli in Experiment 1. *Conflict of Interest*: None declared.

Address correspondence to Andrey R. Nikolaev. Email: nikolaev@brain.riken.jp.

References

Arieli A, Sterkin A, Grinvald A, Aertsen A. 1996. Dynamics of ongoing activity: explanation of the large variability in evoked cortical responses. Science. 273:1868–1871.

Barrie JM, Freeman WJ, Lenhart MD. 1996. Spatiotemporal analysis of prepyriform, visual, auditory, and somesthetic surface EEGs in trained rabbits. J Neurophysiol. 76:520–539.

Barry RJ, Kirkaikul S, Hodder D. 2000. EEG alpha activity and the ERP to target stimuli in an auditory oddball paradigm. Int J Psychophysiol. 39:39–50.

Basar E. 1999. Dynamics of potentials from invertebrate brain. In: Basar E, editor. Brain functions and oscillations II: Integrative brain function. Neurophysiology and cognitive processes. Berlin: Springer. p. 91–108.

Brandt ME, Jansen BH, Carbonari JP. 1991. Pre-stimulus spectral EEG patterns and the visual evoked response. Electroencephalogr Clin Neurophysiol. 80:16–20.

Coles SG, Tawn JA. 1991. Modeling extreme multivariate events. J R Stat Soc Series B Stat Methodol. 53:377–392.

David O, Cosmelli D, Friston KJ. 2004. Evaluation of different measures of functional connectivity using a neural mass model. Neuroimage. 21:659–673.

Delorme A, Makeig S. 2004. EEGLAB: an open source toolbox for analysis of single-trial EEG dynamics including independent component analysis. J Neurosci Methods. 134:9–21.
Ditzinger T, Haken H. 1990. The impact of fluctuations on the recognition of ambiguous patterns. Biol Cybern. 63:453–456.
Fell J. 2007. Cognitive neurophysiology: beyond averaging. Neuroimage. 37:1069–1072.
Fell J, Ludowig E, Rosburg T, Axmacher N, Elger CE. 2008. Phase-locking within human mediotemporal lobe predicts memory formation. Neuroimage. 43:410–419.
Freeman WJ. 2005. Origin, structure, and role of background EEG activity. Part 3. Neural frame classification. Clin Neurophysiol. 116:1118–1129.
Freeman WJ. 2007. Indirect biological measures of consciousness from field studies of brains as dynamical systems. Neural Netw. 20:1021–1031.
Freeman WJ, Baird B. 1987. Relation of olfactory EEG to behavior: spatial analysis. Behav Neurosci. 101:393–408.
Freeman WJ, Barrie JM. 2000. Analysis of spatial patterns of phase in neocortical gamma EEGs in rabbit. J Neurophysiol. 84:1266–1278.
Freeman WJ, Burke BC, Holmes MD. 2003. Aperiodic phase re-setting in scalp EEG of beta-gamma oscillations by state transitions at alpha-theta rates. Hum Brain Mapp. 19:248–272.
Fries P. 2005. A mechanism for cognitive dynamics: neuronal communication through neuronal coherence. Trends Cogn Sci. 9:474–480.
Friston KJ. 2000. The labile brain I: Neuronal transients and nonlinear coupling. Philos Trans R Soc Lond B Biol Sci. 355:215–236.
Galambos R. 1992. A comparison of certain gamma band (40 Hz) brain rhythms in cat and man. In: Basar E, Bullock TH, editors. Induced rhythms in the brain. Boston: Birkhauser. p. 201–216.
Geissler HG. 1987. The temporal architecture of central information processing: evidence for a tentative time-quantum model. Psychol Res. 49:99–106.
Gong P, Nikolaev AR, van Leeuwen C. 2003. Scale-invariant fluctuations of the dynamical synchronization in human brain electrical activity. Neurosci Lett. 336:33–36.
Gong P, Nikolaev AR, van Leeuwen C. 2007. Intermittent dynamics underlying the intrinsic fluctuations of the collective synchronization patterns in electrocortical activity. Phys Rev E Stat Nonlin Soft Matter Phys. 76:011904.
Gross J, Schmitz F, Schnitzler I, Kessler K, Shapiro K, Hommel B, Schnitzler A. 2004. Modulation of long-range neural synchrony reflects temporal limitations of visual attention in humans. Proc Natl Acad Sci USA. 101:13050–13055.
Gruber WR, Klimesch W, Sauseng P, Doppelmayr M. 2005. Alpha phase synchronization predicts P1 and N1 latency and amplitude size. Cereb Cortex. 15:371–377.
Hanslmayr S, Klimesch W, Sauseng P, Gruber W, Doppelmayr M, Freunberger. 1987. Parameter and quantile estimation for the generalized Pareto distribution. Technometrics. 29:339–349.
Ito J, Nikolaev AR, van Leeuwen C. 2005. Spatial and temporal structure of phase synchronization of spontaneous alpha EEG activity. Biol Cybern. 92:54–60.
Ito J, Nikolaev AR, van Leeuwen C. 2007. Dynamics of spontaneous transitions between global brain states. Hum Brain Mapp. 28:904–913.
Klimesch W, Hanslmayr S, Sauseng P, Gruber WR. 2006. Distinguishing the evoked response from phase reset: a comment to Makinen et al. Neuroimage. 29:808–811.
Klimesch W, Hanslmayr S, Sauseng P, Gruber WR, Doppelmayr M. 2007. P1 and traveling alpha waves: evidence for evoked oscillations. J Neurophysiol. 97:1311–1318.
Klimesch W, Sauseng P, Hanslmayr S. 2007. EEG alpha oscillations: the inhibition-timing hypothesis. Brain Res Rev. 53:63–88.
Knyazeva MG, Fornari E, Meuli R, Innocenti G, Maeder P. 2006. Imaging of a synchronous neuronal assembly in the human visual brain. Neuroimage. 29:593–604.
Knyazeva MG, Kiper DC, Vildavski VY, Despland PA, Maeder-Ingvar M, Innocenti GM. 1999. Visual stimulus-dependent changes in interhemispheric EEG coherence in humans. J Neurophysiol. 82:3095–3107.
Kopell N, Ermentrout GB, Whittington MA, Traub RD. 2000. Gamma rhythms and beta rhythms have different synchronization properties. Proc Natl Acad Sci USA. 97:1867–1872.
Kotz S, Nadarajah S. 2000. Extreme value distributions: theory and applications. London: Imperial College Press. p. 185.
Kravitz AV, Peoples LL. 2008. Background firing rates of orbitofrontal neurons reflect specific characteristics of operant sessions and modulate phasic responses to reward-associated cues and behavior. J Neurosci. 28:1009–1018.
Kristofferson AB. 1967. Successiveness discrimination as a two-state, quantal process. Science. 158:1337–1339.
Kubovy M. 1994. The perceptual organization of dot lattices. Psychon Bull Rev. 1:182–190.
Kubovy M, Holcombe AO, Wagemans J. 1998. On the lawfulness of grouping by proximity. Cogn Psychol. 35:71–98.
Kubovy M, Wagemans J. 1995. Grouping by proximity and multistability in dot lattices: a quantitative gestalt theory. Psychol Sci. 6:225–234.
Lachaux JP, Rodriguez E, Martinerie J, Varela FJ. 1999. Measuring phase synchrony in brain signals. Hum Brain Mapp. 8:194–208.
Lachaux JP, Rodriguez E, Van Quyen ML, Lutz A, Martinerie J, Varela FJ. 2000. Studying single-trials of phase synchronous activity in the brain. Int J Bifurcat Chaos. 10:2429–2439.
Lalanne L. 1876. Sur la duree de la sensation tactile [on the duration of tactile sensations]. Note C R Acad Sci Paris. 39:1314–1316.
Lichtenstein M. 1961. Phenomenal simultaneity with irregular timing of components of the visual stimulus. Percept Mot Skills. 12:47–60.
Linkenkaer-Hansen K, Nikouline VV, Palva JM, Ilmoniemi RJ. 2001. Long-range temporal correlations and scaling behavior in human brain oscillations. J Neurosci. 21:1370–1377.
Linkenkaer-Hansen K, Nikulin VV, Palva JM, Kaila K, Ilmoniemi RJ. 2004. Stimulus-induced change in long-range temporal correlations and scaling behaviour of sensorimotor oscillations. Eur J Neurosci. 19:203–211.
Livanov MN. 1977. Spatial organization of cerebral processes. New York: John Wiley & Sons. p. 190.
Makeig S, Westerfield M, Jung TP, Enghoff S, Townsend J, Courchesne E, Sejnowski TJ. 2002. Dynamic brain sources of visual evoked responses. Science. 295:690–694.
Mudholkar GS, Srivastava DK. 1993. Exponentiated Weibull family for analyzing bathtub failure-rate data. IEEE Trans Reliab. 42: 299–302.
Nakatani C, Ito J, Nikolaev AR, Gong P, van Leeuwen C. 2005. Phase synchronization analysis of EEG during attentional blink. J Cogn Neurosci. 17:1969–1979.
Nikolaev AR, Gepshtein S, Kubovy M, van Leeuwen C. 2007. Temporal structure of perceptual grouping: EEG analysis. In: Mori S, Miyaoka T, Wong W, editors. Proceedings of the 23rd Annual Meeting of the International Society for Psychophysics (Fechner Day); October 20–23, 2007; Tokyo (Japan): The International Society of Psychophysics. p. 67–72.
Nikolaev AR, Gepshtein S, Kubovy M, van Leeuwen C. 2008. Dissociation of early evoked cortical activity in perceptual grouping. Exp Brain Res. 186:107–122.
Nikolaev AR, Gong P, van Leeuwen C. 2005. Evoked phase synchronization between adjacent high-density electrodes in human scalp EEG: duration and time course related to behavior. Clin Neurophysiol. 116:2403–2419.
Ohl FW, Scheich H, Freeman WJ. 2001. Change in pattern of ongoing cortical activity with auditory category learning. Nature. 412:733–736.
Palva S, Palva JM. 2007. New vistas for alpha-frequency band oscillations. Trends Neurosci. 30:150–158.
Parker AJ, Newsome WT. 1998. Sense and the single neuron: probing the physiology of perception. Annu Rev Neurosci. 21:227–277.
Pfurtscheller G, Aranibar A. 1977. Event-related cortical desynchronization detected by power measurements of scalp EEG. Electroencephalogr Clin Neurophysiol. 42:817–826.
Pfurtscheller G, Neuper C, Mohl W. 1994. Event-related desynchronization (ERD) during visual processing. Int J Psychophysiol. 16:147–153.
Quian Quiroga R, Kraskov A, Kreuz T, Grassberger P. 2002. Performance of different synchronization measures in real data: a case study on electroencephalographic signals. Phys Rev E Stat Nonlin Soft Matter Phys. 65:041903.

Romei V, Brodbeck V, Michel C, Amedi A, Pascual-Leone A, Thut G. 2007. Spontaneous fluctuations in posterior alpha-band EEG activity reflect variability in excitability of human visual areas. Cereb Cortex. doi: 10.1093/cercor/bhm229.

Rosenblum M, Pikovsky A, Kurths J, Schafer C, Tass P. 2001. Phase synchronization: from theory to data analysis. In: Moss F, Gielen S, editors. Neuro-informatics, handbook of biological physics. New York: Elsevier. p. 279–321.

Sannita WG. 2000. Stimulus-specific oscillatory responses of the brain: a time/frequency-related coding process. Clin Neurophysiol. 111:565–583.

Sannita WG, Lopez L, Piras C, Di Bon G. 1995. Scalp-recorded oscillatory potentials evoked by transient pattern-reversal visual stimulation in man. Electroencephalogr Clin Neurophysiol. 96:206–218.

Singer W. 1999. Time as coding space? Curr Opin Neurobiol. 9:189–194.

Stam CJ, Breakspear M, van Cappellen van Walsum AM, van Dijk BW. 2003. Nonlinear synchronization in EEG and whole-head MEG recordings of healthy subjects. Hum Brain Mapp. 19:63–78.

Stroud JM. 1955. The fine structure of psychological time. In: Quasten H, editor. Information theory in psychology. Glencoe (IL): Free Press. p. 174–207.

Supp GG, Schlogl A, Fiebach CJ, Gunter TC, Vigliocco G, Pfurtscheller G, Petsche H. 2005. Semantic memory retrieval: cortical couplings in object recognition in the N400 window. Eur J Neurosci. 21:1139–1143.

Tallon-Baudry C, Bertrand O. 1999. Oscillatory gamma activity in humans and its role in object representation. Trends Cogn Sci. 3:151–162.

Tallon-Baudry C, Bertrand O, Delpuech C, Pernier J. 1996. Stimulus specificity of phase-locked and non-phase-locked 40 Hz visual responses in human. J Neurosci. 16:4240–4249.

Tallon-Baudry C, Bertrand O, Fischer C. 2001. Oscillatory synchrony between human extrastriate areas during visual short-term memory maintenance. J Neurosci. 21:RC177.

Tass P, Rosenblum MG, Weule J, Kurths J, Pikovsky A, Volkmann J, Schnitzler A, Freund HJ. 1998. Detection of n:m phase locking from noisy data: application to magnetoencephalography. Phys Rev Lett. 81:3291–3294.

Tyukin IY, Prokhorov D, van Leeuwen C. 2008. Adaptive classification of temporal signals in fixed-weights recurrent neural networks: an existence proof. Neural Comput. 20:2564–2596.

van der Helm PA. 2006. Book review of F. Sundqvist (2003) "Perceptual Dynamics". Philos Psychol. 19:267–279.

van Leeuwen C. 2007. What needs to emerge to make you conscious? J Conscious Stud. 14:115–136.

van Leeuwen C, Bakker L. 1995. Stroop can occur without Garner interference: strategic and mandatory influences in multidimensional stimuli. Percept Psychophys. 57:379–392.

van Leeuwen C, Steyvers M, Nooter M. 1997. Stability and intermittency in large-scale coupled oscillator models for perceptual segmentation. J Math Psychol. 41:319–344.

van Leeuwen C, van den Hof M. 1991. What has happened to Prägnanz? Coding, stability, or resonance. Percept Psychophys. 50:435–448.

VanRullen R, Koch C. 2003. Is perception discrete or continuous? Trends Cogn Sci. 7:207–213.

Varela F, Lachaux JP, Rodriguez E, Martinerie J. 2001. The brainweb: phase synchronization and large-scale integration. Nat Rev Neurosci. 2:229–239.

von der Malsburg C. 1985. Nervous structures with dynamical links. Ber Bunsenges Phys Chem. 89:703–710.

von Stein A, Rappelsberger P, Sarnthein J, Petsche H. 1999. Synchronization between temporal and parietal cortex during multimodal object processing in man. Cereb Cortex. 9:137–150.

von Stein A, Sarnthein J. 2000. Different frequencies for different scales of cortical integration: from local gamma to long range alpha/theta synchronization. Int J Psychophysiol. 38:301–313.

von Uexkuell J. 1928. Theoretische biologie [theoretical biology]. Berlin (Germany): Springer.

Wertheimer M. 1912. Experimentelle Studien über das Sehen von Bewegung. Z Psychol. 61:161–265.

Yeung N, Bogacz R, Holroyd CB, Cohen JD. 2004. Detection of synchronized oscillations in the electroencephalogram: an evaluation of methods. Psychoph. 41:822–832.